iScience

CellPress
OPEN ACCESS

Article

Interactions between fungal hyaluronic acid and host CD44 promote internalization by recruiting host autophagy proteins to forming phagosomes

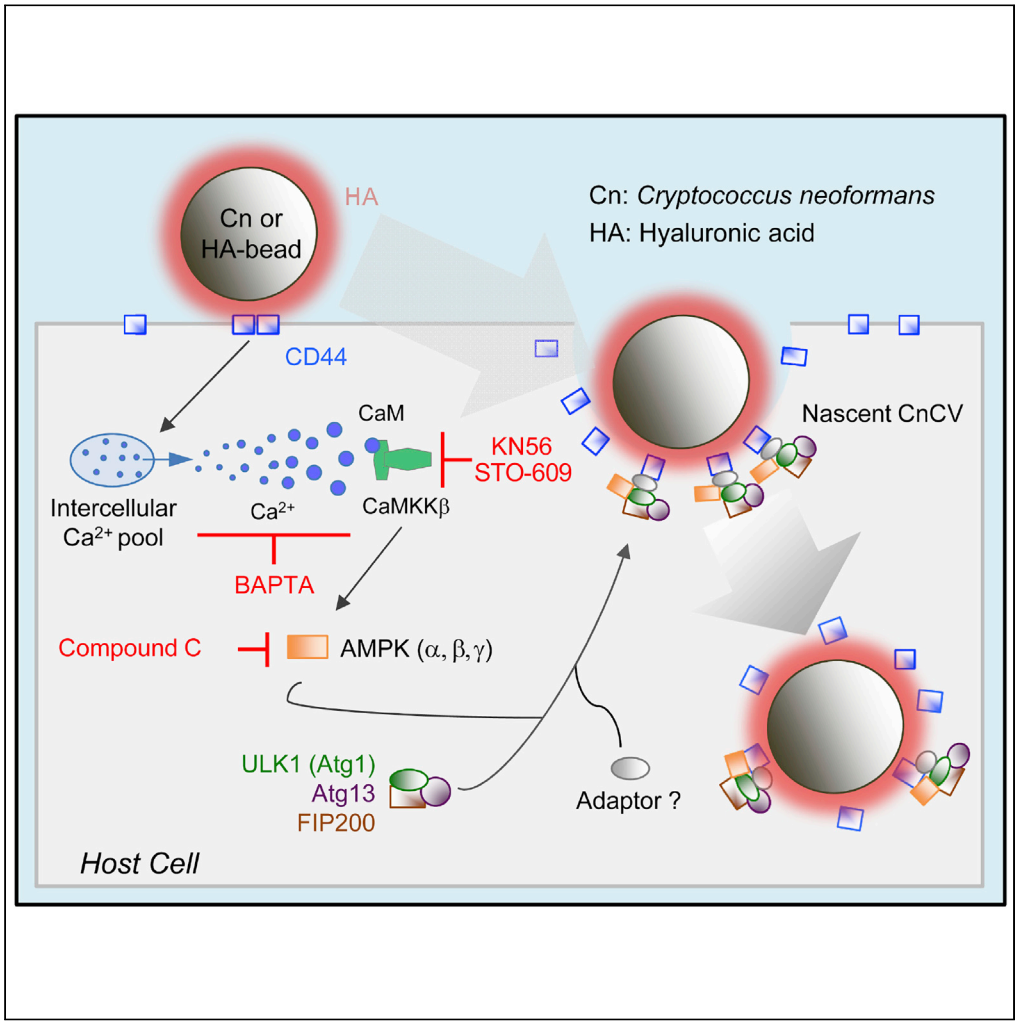

Shengli Ding, Jing Yang, Xuehuan Feng, ..., Qing-Ming Qin, Thomas A. Ficht, Paul de Figueiredo

qmqin@jlu.edu.cn (Q.-M.Q.)
tficht@cvm.tamu.edu (T.A.F.)
pjdefigueiredo@tamu.edu (P.d.F.)

HIGHLIGHTS

Fungal HA drives non-canonical and ligand-induced autophagy in phagocytic cells

Cn recruits host CD44 to forming phagocytic cups to initiate fungal internalization

Fungal HA-CD44 interactions elevate intracellular Ca^{2+} levels and activate CaMKKβ

A Ca^{2+}-CaMKKβ-AMPK-ULK1 signaling axis is involved in HA-CD44 induced autophagy

Ding et al., iScience 24, 102192
March 19, 2021
https://doi.org/10.1016/j.isci.2021.102192

iScience

CellPress
OPEN ACCESS

Article

Interactions between fungal hyaluronic acid and host CD44 promote internalization by recruiting host autophagy proteins to forming phagosomes

Shengli Ding,[1,2,6,7] Jing Yang,[2,7] Xuehuan Feng,[2,7] Aseem Pandey,[2,3] Rola Barhoumi,[4] Dongmei Zhang,[2] Samantha L. Bell,[2] Yue Liu,[1] Luciana Fachini da Costa,[2,5] Allison Rice-Ficht,[5] Robert O. Watson,[2] Kristin L. Patrick,[2] Qing-Ming Qin,[1,2,*] Thomas A. Ficht,[3,*] and Paul de Figueiredo[2,3,8,*]

SUMMARY

Phagocytosis and autophagy play critical roles in immune defense. The human fungal pathogen *Cryptococcus neoformans* (Cn) subverts host autophagy-initiation complex (AIC)-related proteins, to promote its phagocytosis and intracellular parasitism of host cells. The mechanisms by which the pathogen engages host AIC-related proteins remain obscure. Here, we show that the recruitment of host AIC proteins to forming phagosomes is dependent upon the activity of CD44, a host cell surface receptor that engages fungal hyaluronic acid (HA). This interaction elevates intracellular Ca^{2+} concentrations and activates CaMKKβ and its downstream target AMPKα, which results in activation of ULK1 and the recruitment of AIC components. Moreover, we demonstrate that HA-coated beads efficiently recruit AIC components to phagosomes and CD44 interacts with AIC components. Taken together, these findings show that fungal HA plays a critical role in directing the internalization and productive intracellular membrane trafficking of a fungal pathogen of global importance.

INTRODUCTION

Autophagy is an orderly "self-eating" process in cells that coordinates the degradation of cellular components. Various types of autophagy have been described, including macrophagy, microphagy, mitophagy, chaperone-mediated autophagy and xenophagy (Galluzzi et al., 2017; Khandia et al., 2019; Kirkin and Rogov, 2019). Some pathogens subvert autophagic machinery to promote their intracellular survival and replication (Case et al., 2016; de Figueiredo and Dickman, 2016; de Figueiredo et al., 2015; Dickman et al., 2017; Pandey et al., 2018). Several signaling pathways control the onset, duration and outcome of autophagy induction in mammalian cells (Abada and Elazar, 2014; Rubinsztein et al., 2012). Pathways that include components of the autophagy initiation complex (AIC), including AMPK, ULK1, ATG13, FIP200 and ATG9, play important roles in these processes (Ganley et al., 2009; Hosokawa et al., 2009; Jung et al., 2009). For example, AMPK or ULK1 signaling can regulate ATG9 recruitment to nascent phagosome or autophagosome membranes (Mack et al., 2012). This recruitment process is believed to contribute to the elongation of the autophagosomal membrane (Mack et al., 2012).

Cryptococcus neformans (Cn) is a pathogen of global consequence that causes fatal fungal meningoencephalitis worldwide (Kozubowski and Heitman, 2012; Olszewski et al., 2010; Sabiiti and May, 2012). Cn is particularly pernicious in immunocompromised individuals, where lethal infection constitutes a significant risk (Warkentien and Crum-Cianflone, 2010). Cn can survive, replicate and persist in both intracellular and extracellular environments within mammalian hosts (Garcia-Rodas and Zaragoza, 2012). However, the molecular mechanisms that control intracellular parasitism remain poorly understood (Evans et al., 2018; Zaragoza, 2019). Toward addressing this issue, we reported a functional analysis of host factors that regulate the infection, intracellular replication, and non-lytic release of Cn from host cells (Qin et al., 2011). We extended these findings by performing a phosphoproteomic analysis of the host response to Cn infection (Pandey et al., 2017). This analysis demonstrated that host AIC proteins, and upstream regulatory molecules, contribute to the internalization and intracellular replication of the pathogen in macrophages

[1]College of Plant Sciences & Key Laboratory of Zoonosis Research, Ministry of Education, Jilin University, Changchun, Jilin 130062, China

[2]Department of Microbial Pathogenesis and Immunology, Texas A&M Health Science Center, Bryan, TX 77807, USA

[3]Department of Veterinary Pathobiology, Texas A&M University, College Station, TX 77843, USA

[4]Department of Veterinary Integrative Biosciences, Texas A&M University, College Station, TX 77843-4458, USA

[5]Department of Molecular and Cellular Medicine, College of Medicine, Texas A&M Health Science Center, College Station, TX 77843, USA

[6]Department of Plant Pathology, College of Plant Protection, Henan Agricultural University, Zhengzhou, Henan 450002, China

[7]These authors contributed equally

[8]Lead Contact

*Correspondence: qmqin@jlu.edu.cn (Q.-M.Q.), tficht@cvm.tamu.edu (T.A.F.), pjdefigueiredo@tamu.edu (P.d.F.)

https://doi.org/10.1016/j.isci.2021.102192

(Pandey et al., 2017). This work also raised questions about the cellular and molecular mechanisms by which these proteins contribute to this phenotype.

The internalization of Cn into host cells is regulated, in part, by interactions between fungal components and host associated CD44, a major receptor for hyaluronic acid (HA) in mammalian cells (Jong et al., 2008, 2012). Moreover, CD44 has been shown to control phagocytosis of the pathogen (Jong et al., 2008, 2012). Interestingly, mice deficient for CD44 display reduced susceptibility to infection (Jong et al., 2012). The deficiency in phagocytosis accounts for this phenotype, leaving open the question of the mechanism by which CD44 controls fungal internalization. Here, we show that Cn phagocytosis by macrophages occurs by a novel mechanism whereby AIC proteins, including ULK1, ATG9 and ATG13, as well as the key upstream signaling component AMPKα, are recruited to forming phagosomes to promote the phagocytosis of the pathogen in a CD44-dependent fashion. Interaction of fungal HA and host CD44 activates a Ca^{2+}-CaMKKβ (calcium/calmodulin-dependent protein kinase kinase β subunit)-AMPK-ULK1 signaling axis that supports Cn internalization into host cells. Taken together, our findings uncover unexpected roles for HA-CD44 interactions in conferring susceptibility to fungal infection and open up new avenues for therapeutic intervention for a fungal pathogen of global importance.

RESULTS

Cn recruits host AIC components to forming Cn-containing phagosomes

To test the hypothesis that Cn infection of macrophages promotes the formation of a physical complex that contains AIC components, we used Förster Resonance Energy Transfer (FRET) imaging microscopy, which detects close molecular associations (<10 nm) (Irving et al., 2014), to measure such interactions. The quenching of fluorescence in the donor fluorophore of an FRET pair accompanies the establishment of a close physical association between the pairs (Irving et al., 2014). We measured photon transfer between antibody labeled ATG13 and ULK1 or AMPKα and FIP200 in infected and uninfected RAW264.7 macrophages. We observed significant increases in the amount of FRET between these proteins in infected cells (Figures S1A–S1D). However, comparable FRET interactions were not observed in controls that were stained with a single label, or in uninfected samples (Figures S1A–S1D), thereby indicating the establishment of a close association between these proteins during infection.

Recruitment of AIC components to forming phagosomes containing Cn is galectin 8 independent

Previous studies have shown that galectin 8, a β-galactoside-binding lectin, monitors endosomal and lysosomal integrity by binding to host glycans on damaged pathogen-containing vacuoles. This binding drives the ubiquitin-dependent recruitment of autophagy adaptor proteins (e.g., NDP52) and microtubule associated light chain kinase 3 (LC3), which in turn, promotes the recruitment of autophagosome biogenesis proteins to damaged pathogen-containing vacuoles (Thurston et al., 2012). Galectin 8 mediated autophagosomal targeting is relevant to the observed recruitment of AIC components to phagocytic cups because Cn containing vacuoles (CnCVs) are permeabilized after phagocytosis by macrophages (Johnston and May, 2010). Moreover, nascent CnCVs in infected macrophages recruit host LC3 (Figure S1E) (Nicola et al., 2012; Qin et al., 2011), thereby implicating trafficking pathways that recruit LC3 to phagosomal membranes in controlling the intracellular lifestyle of Cn. With these ideas in mind, we tested the hypothesis that AIC recruitment to nascent CnCVs is associated with galectin 8 recruitment to these subcellular structures. We infected RAW264.7 macrophages that express a GFP-tagged variant of galectin 8 (GFP-Gal8) with Cn, and then used immunofluorescence microscopy (IFM) to determine whether GFP-Gal8 colocalized with AMPKα on nascent phagosomes containing Cn cells. We found that GFP-Gal8 did not display quantitative colocalization with either AMPKα or nascent phagosomes (Figure S1F). Consistent with these observations was the finding that UBEI-41, a potent and cell-permeable inhibitor of ubiquitin E1 activity (Yang et al., 2007), when added to macrophages at non-toxic doses (30 μM), did not diminish AMPKα recruitment to CnCVs (Figure S1G). Importantly, the inhibitor was washed out of the host cell culture media before Cn infection, thereby ensuring that the drug only targeted host cell components in these experiments. In addition, we found that nascent phagosomes decorated with the AIC component ULK1 colocalized with the endosomal marker EEA1 (Figure S1H). We also found that LC3 displayed minimal colocalization with AIC components on nascent CnCVs (Figure S1I). CnCVs in B6J2 macrophages expressing dominant negative variants of the AIC regulatory component AMPKα recruited less LC3 (Figure S1J) and AIC components (Figure S1K), thereby suggesting that AIC recruitment to nascent Cn-containing phagosomes and LC3 recruitment to phagosome membranes could be morphologically and genetically dissected. Taken together, these findings indicated that recruitment of AIC to the nascent phagosomes and the induction of autophagy were galectin 8-independent events.

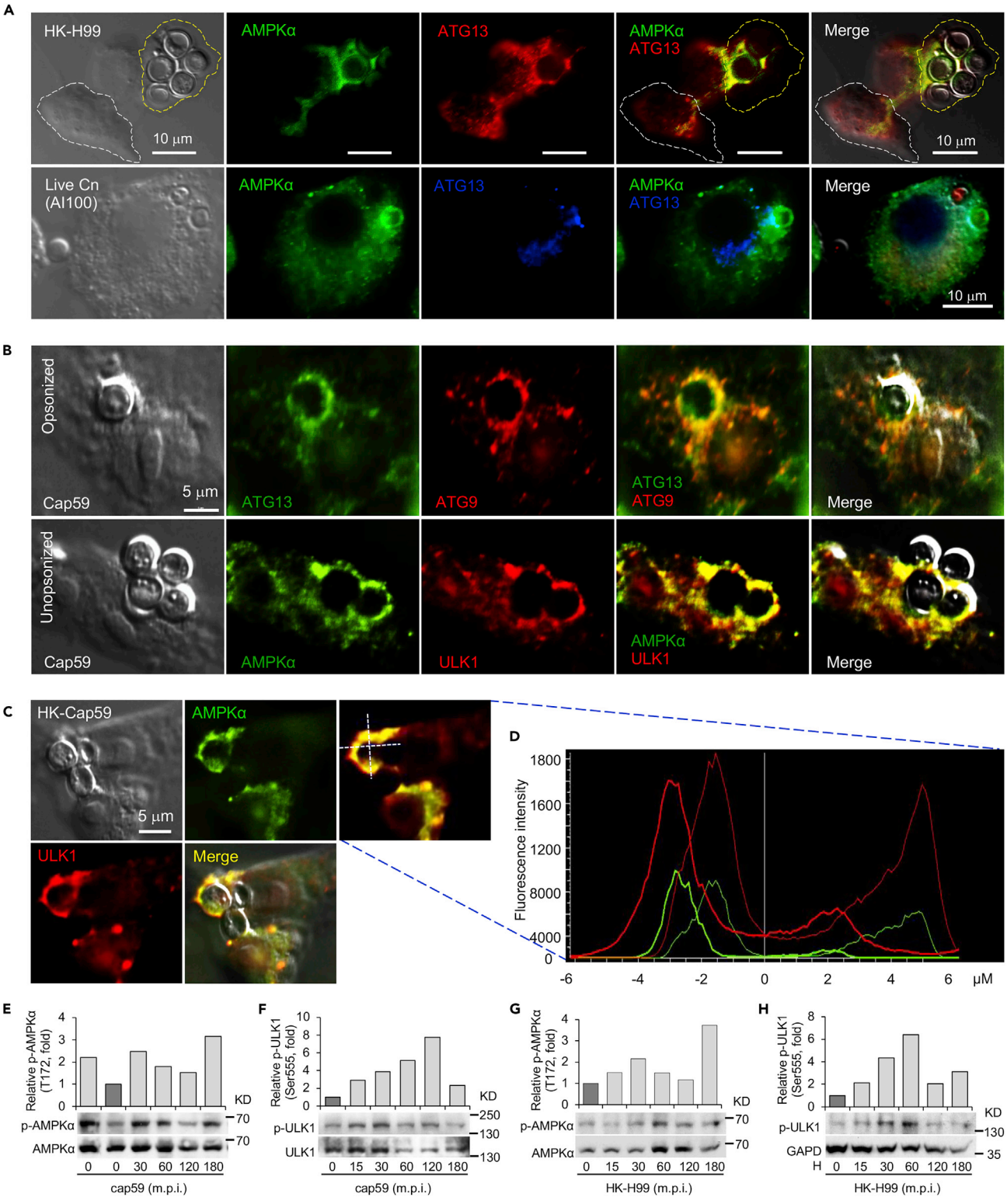

Figure 1. Non-proteineous components on *Cryptococcus neoformans* (Cn) direct the recruitment of host AIC components to nascent phagosomes

(A and B) Colocalization of AMPKα and AIC components surrounding nascent CnCVs in host cells infected with live or heat-killed (HK) H99 (A) and opsonized or unopsonized acapsular cap59 strains (B) of Cn. RAW264.7 macrophages were infected with the indicated Cn cells at a multiplicity of infection (MOI) of 5. At 3 hr post infection (h.p.i.), the infected cells were fixed with 3.7% formaldehyde in 1×PBS for 1 to 2 hr and then subjected to immunofluorescence microscopy

Figure 1. *Continued*
assays with the indicated antibodies. Host cells bounded with yellow or white dash lines indicate cells containing or lacking internalized Cn cells, respectively.
(C and D) Recruitment of AMPKα and ULK1 to nascent CnCVs in host cells incubated with HK-cap59 (5 MOI) at 3 h.p.i. (C) and the fluorescence intensity profile of AMPKα (green) and ULK1 (red) along the two crossed white lines (D).
(E and F) Activation of host cell AMPKα (E) and ULK1 (F) by acapsular Cn strain cap59. Representative blots and data from one of three independent experiments are shown in (E to H).
(G and H) Activation of host cell AMPKα (G) and ULK1 (H) by HK Cn strain H99 (HK-H99).

A non-proteinaceous and/or non-capsular component controls AIC recruitment to nascent CnCVs

The observation that AIC and AIC regulatory components were recruited to forming phagosomes during Cn infection of macrophages encouraged us to determine the mechanism of recruitment. We infected host cells with live or heat-killed (HK) Cn and found that fungal viability was not required for AIC recruitment because nascent CnCVs containing the HK organism also efficiently recruited these proteins (Figure 1A). However, compared to host cells with internalized Cn cells, differential expression or fluorescence signal levels as well as differential localization of AIC and AIC regulatory components in host cells lacking Cn cells were observed (Figures 1A, S1F–S1G, S1J, and S2). These observations were consistent with the hypothesis that non-proteinaceous, Cn-associated molecules activate the host AIC pathway.

Cn is encased in a carbohydrate-enriched capsule that is essential for intracellular parasitism and virulence (O'Meara and Alspaugh, 2012). To test the hypothesis that capsular components direct the recruitment of AIC and AIC regulatory proteins to forming phagosomes, we infected host cells with an acapsular mutant of Cn (Cap59), which displays defects in extracellular trafficking of glucuronoxylomannan (GXM) (Garcia-Rivera et al., 2004), and analyzed AIC recruitment to phagosomes containing cap59 strains. We found that forming and formed phagosomes that contained the acapsular strain also efficiently recruited AIC proteins (Figures 1B–1D and S3A–S3C). AIC components showed close associations with internalized Cn cells as detected by indirect immunofluorescence with the monoclonal antibody 18B7 against GXM (Garcia-Rivera et al., 2004) (Figure S3D). Moreover, infection of host cells with live wild-type (WT) Cn resulted in the activation by phosphorylation of host cell ULK1 (Ser555), a key component of the AIC, and activation of the AIC regulatory protein AMPKα (Thr172) (Pandey et al., 2017). Similarly, the acapsular mutant and HK Cn also activated host AMPKα (Thr172) and/or ULK1 (Figures 1E–1H and S3E). However, when *S. cerevisiae* was incubated with host cells, similar AIC recruitment was not observed (Figure S3F), suggesting that phagocytosis of yeast cells by macrophages involves the participation of a distinct mechanism. Taken together, these findings suggested that Cn-specific, non-proteinaceous, non-capsular components activated the host AMPK-ULK1 signaling axis and promoted AIC recruitment to forming phagosomes.

CD44-deficient host cells fail to recruit AIC proteins to forming phagosomes

CD44 regulates fungal internalization (Jong et al., 2008, 2012). This observation raised the intriguing possibility that CD44 interactions with other host cell components may also control the recruitment of AIC components to nascent CnCVs. To test this hypothesis, we first used fluorescence microscopy to determine whether CD44 colocalized with Cn cells or was recruited to forming or formed nascent CnCVs. We also tested whether CD44 deficient macrophages recruited AIC components to the nascent pathogen-containing phagosomes. We found that forming or formed phagosomes containing both capsular or acapsular strains displayed strong colocalization with CD44 (Figure 2A), and that CD44 was enriched at sites of contact between the pathogen and the host cell surface during a time course of infection (Figure S3G). Next, we tested whether CD44 colocalized with AIC regulatory AMPK and AIC components on nascent CnCVs. We found that AIC components, including ATG9 and ULK1, colocalized with CD44 on nascent CnCVs (Figures 2B and 2C). Compared to $CD44^{+/+}$ bone-marrow derived macrophage (BMDM) controls, AMPKα showed reduced colocalization in $CD44^{-/-}$ BMDMs (Figure 2D). As a result, Cn internalization in CD44-deficient cells was reduced (Figures 2E and 2F), indicating that host cell CD44 is required for Cn internalization, and suggesting that activation of the AMPK-ULK1 signaling axis and AIC recruitment is CD44-dependent.

cps1 deletion mutants fail to recruit AIC components to nascent CnCVs

HA, a component of the Cn cell wall, is known to interact with CD44, an HA receptor on host cells, and to promote the internalization of the pathogen into human and murine brain microvascular endothelial cells (BMECs) (Jong et al., 2008, 2012). This observation raised the intriguing possibility that HA-CD44 interactions may promote the recruitment of AIC components to nascent CnCVs. To test this hypothesis, we first examined the

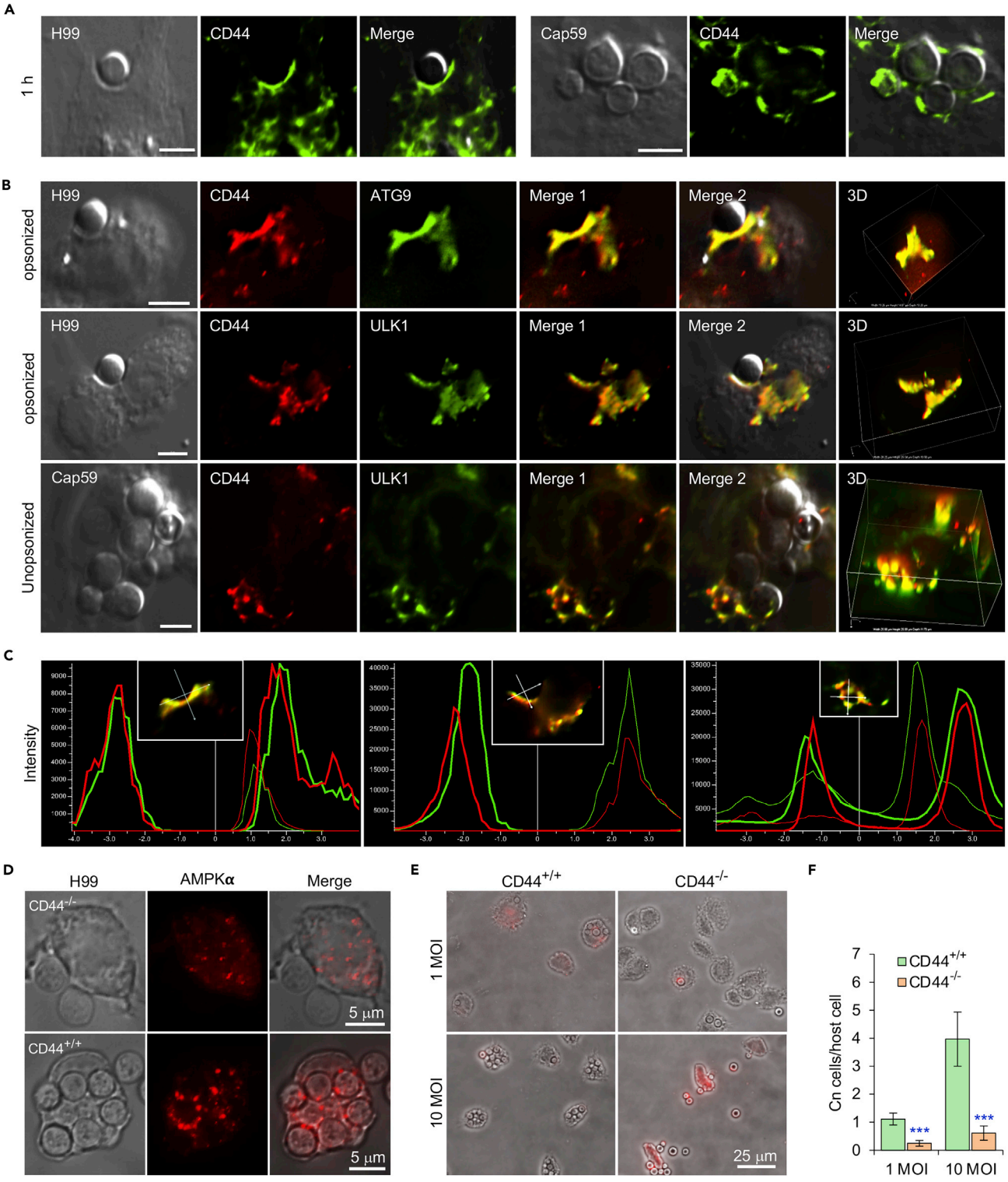

Figure 2. Host-associated CD44 is required for Cn host cell internalization

(A) Recruitment of host CD44 to nascent CnCVs that contained the wild-type (WT) strain H99 (leaf panel) or acapsular mutant strain cap59 (right panel) of Cn. At 1 h.p.i., host cells were fixed, permeabilized and processed for immunofluorescence microscopy using antibodies directed against the indicated host proteins. The antibody-stained samples were then subjected to confocal microscopy image analysis. Bars: 5 μm.

(B) Colocalization of CD44 with the indicated AIC components in the vicinity of nascent CnCVs in host cells infected with the indicated Cn strains. Bars: 5 μm.

Figure 2. *Continued*

(C) The fluorescence intensity profile of CD44 (red) and AIC components (ATG9 or ULK1) (green) along the two crossed white lines shown in the insets from (B, Merge 1).

(D) AMPK recruitment to nascent CnCVs in CD44 knockout (KO, $CD44^{-/-}$) and WT ($CD44^{+/+}$) bone marrow-derived macrophages (BMDMs) at 3 h.p.i.

(E and F) Cn internalization in CD44 WT and KO BMDMs infected by Cn H99 (1 or 10 MOI) assessed using image analysis approaches (E) and corresponding quantification (F) at 3 h.p.i. Data represent the means ± standard error of mean (SEM) from three independent experiments. ***: significance at $p < 0.001$.

internalization of Cn strains that harbor mutations in *cps1*, a gene that encodes hyaluronic synthase (Jong et al., 2007). Consistent with previous findings where Cn displayed reduced association with CD44-depleted murine BMECs compared to controls (Jong et al., 2012), we found that deletion of *cps1* displayed reduced internalization of Cn into host macrophages (Figures 3A–3C and S4A). Next, we used fluorescence microscopy to determine whether *cps1*-deficient Cn strains recruited AIC components to nascent pathogen-containing phagosomes. We found the mutant strain displayed reduced recruitment compared to WT controls (Figure 3D). However, nascent CnCVs that contained strain C558 (*cps1*Δ::*CPS1*), in which the *cps1* mutation was complemented with a WT copy of the gene (Jong et al., 2008), displayed higher levels of AIC recruitment than their *cps1*-deficient counterparts (Figure 3D, bottom panel). These data suggested that HA, the product of *cps1* activity, contributed to directing the recruitment of AIC components to nascent CnCVs, and implicated a role for CD44, the dominant HA receptor on macrophages, in regulating this process.

Pathogen-derived HA drives interactions between CD44 and AIC components

To test whether HA was sufficient to induce CD44-mediated recruitment of AIC components to nascent CnCVs, we determined whether HA-coated beads induced similar recruitment to forming phagosomes. For these experiments, we covalently coupled HA to polystyrene beads and then incubated the HA-coupled beads with RAW264.7 macrophages for various lengths of time. We also used antibodies directed against AIC components in immunofluorescence microscopy experiments to visualize the recruitment of AIC components to forming phagosomes that contained beads. We found robust recruitment of AMPKα and AIC component ULK1 to forming phagosomes containing HA-coated beads (Figures 3E–3H). We also incubated HA-coated beads with GFP-Gal8 expressing macrophages and found that co-recruitment of AMPKα and galectin 8 to the sites of bead internalization was not detected (Figure S4B, upper). However, co-localization of CD44 and AMPKα was observed to be colocalized with the HA-coated beads (Figure S4B, lower), Our observations therefore suggested that HA interactions with CD44 were necessary and sufficient to induce the formation of an AIC protein complex on forming phagosomes.

Interaction of fungal HA with host CD44 activates AMPK and AIC pathways

The observation that interactions between HA and host CD44 recruited AIC components to forming phagosomes raised questions about the mechanism of AIC recruitment by these components. HA induces Ca^{2+} elevation in cells and may increase the activity of Ca^{2+}-associated signaling pathways (Singleton and Bourguignon, 2002). For example, an increase of cytoplasmic Ca^{2+} levels can induce autophagy through CaMKKβ and AMPK pathways (Feng et al., 2020; Green et al., 2011). To test whether HA and CD44 interactions elevate intracellular Ca^{2+} ($[Ca^{2+}]_i$) levels and induce autophagy by Ca^{2+}-mediated activation of CaMKKβ and AMPK pathways, we incubated host cells with Cn cells, HA or HA-coated beads, and then visualized $[Ca^{2+}]_i$ levels and activation of CaMKKβ-AMPK pathways in the treated cells. We observed that compared to the controls, *cps1*$^+$-Cn induced Ca^{2+}-fluxes and increased $[Ca^{2+}]_i$ concentrations in a pulsed manner (Figures 4A–4C; Videos S1 and S2). Corresponding to the increase of $[Ca^{2+}]_i$ levels, activation of CaMKKβ and AMPKα was observed in host cells incubated with Cn cells (Pandey et al., 2017), HA or HA-coated beads (Figures 4D and 4E). Importantly, phosphorylated AMPKα and ATG9 were co-immunoprecipitated (Co-IP) from host cells incubated with HA-coated, but not naked, beads (Figure 4F). Moreover, during Cn infection, host CD44 expression was induced (Figure 4G) and physical interactions of host CD44 and AIC components, including ATG13 and ATG9, were detected (Figure 4H).

To test whether activation of AMPK resulted from the increase of $[Ca^{2+}]_i$, we treated host cells with or without supplementation of assorted inhibitors, including BAPTA-AM (a $[Ca^{2+}]_i$-chelator), KN62 (a specific CaMK inhibitor), and STO-609 (a specific CaMKKα/β inhibitor), during infection with Cn. We found that host cells treated with these compounds displayed reduced activation of AMPKα (Figure 4I); the activation of the downstream target ULK1 was also almost completely blocked (Figure 4J). During Cn infection, ULK1 is activated in a p-AMPKα-dependent fashion (Figures 4I–4K). Consequently, Cn internalization was reduced in cells in which $[Ca^{2+}]_i$ was chelated, the activities of CaMK or CaMKKα/β were inhibited or depleted (Figures

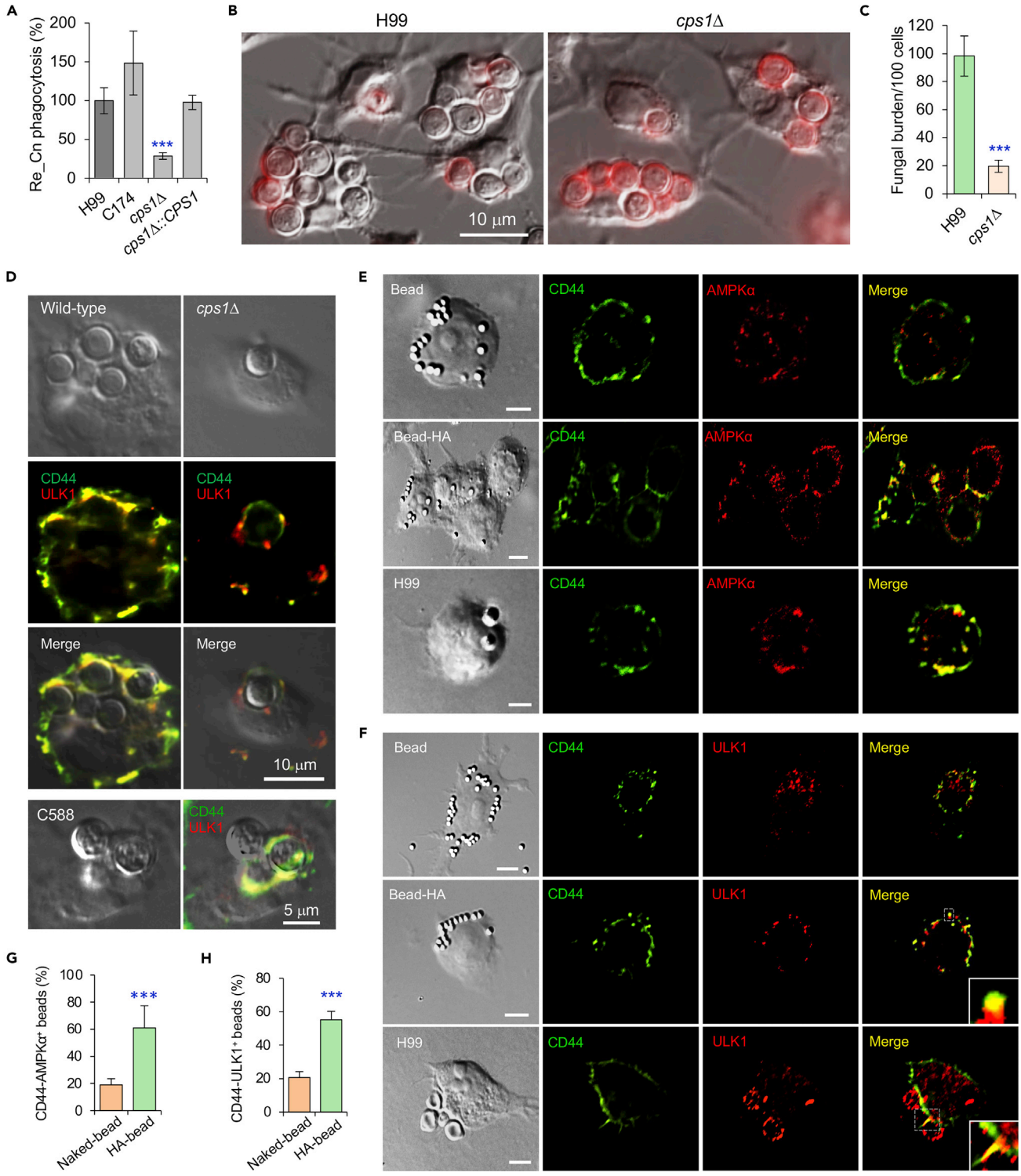

Figure 3. Fungal HA is required for recruitment of AMPK or AIC components to nascent phagosomes and Cn internalization

(A) Internalization of the wild-type, *cps1*Δ and complemented Cn strains via colony formation unit (CFU) assay. Re_Cn: relative Cn.

(B and C) Internalization of the indicated Cn strains in BMDMs (B) and quantification of intracellular Cn cells (C) at 3 h.p.i. via microscopy image analysis. BMDMs were infected with the indicated Cn strains at an MOI of 10.

(D) Confocal microscopy image analysis of recruitment of CD44 and the AIC component ULK1 by wild-type, *cps1*Δ, and complemented (C588) Cn strains (5 MOI for each strain) at 3 h.p.i.

Figure 3. *Continued*
(E and F) Recruitment of host CD44 and AMPKα (E), or CD44 and AIC component ULK1 (F) to nascent phagosomes or CnCVs by HA-coated beads or Cn (H99, 5 MOI), respectively. Bars: 5 μm.
(G and H) Quantification of CD44 and AMPKα positive beads (G) or CD44 and ULK1 positive beads based on confocal microscopy images as shown in (E, F). Data represent the means ± SEM from three independent experiments. ***: significance at $p < 0.001$.

4L and S5A–S5D), or AMPK or AIC components were depleted (Figures S5E and S5F). These findings suggest that interaction of HA with CD44 recruits AIC to forming phagosomes by increase of $[Ca^{2+}]_i$ and activation of the CaMKKβ-AMPK-ULK1 signaling axis.

DISCUSSION

The intracellular lifestyle of Cn is pivotal for pathogen colonization, dissemination and disease progression (Garcia-Rodas and Zaragoza, 2012; Johnston and May, 2013; Seider et al., 2010), as well as establishment of latent infection (Saha et al., 2007). Although the complete set of host factors that regulate intracellular parasitism remain obscure, published reports demonstrate that both "zipper" (receptor-mediated) and "trigger" (membrane ruffle dependent) mechanisms contribute to the internalization of Cn (Guerra et al., 2014). Moreover, interactions between the opsonized or unopsonized pathogen and host cell surface receptors are important to these processes (Shoham et al., 2001; Taborda and Casadevall, 2002). The findings reported here provide a new understanding of phagocytic mechanisms by demonstrating that fungal HA- and host CD44-dependent recruitment of AIC network components to nascent CnCVs play a central role in regulating the internalization of the fungus. Cn cells, opsonized or unopsonized and live or dead, as well as HA-coated beads, efficiently recruited host CD44, components of AIC and its regulatory protein AMPK to forming or formed phagosomes. As such, this report provides the first example of ligand- and receptor-induced recruitment of AIC proteins, including ULK1, FIP200, ATG13, and ATG9, to nascent phagosomes in macrophages.

Host cell galectin 8 is involved in defending against bacterial infection by recruiting the autophagic adaptor NDP52 to damaged *Salmonella*-containing vacuoles and in activating antibacterial autophagy (Thurston et al., 2012). Different from the defensive autophagy induced by galectin 8, significant recruitment of the danger receptor galectin 8 to forming or formed phagosomes during Cn internalization and/or intracellular replication was not observed, suggesting that a different strategy is employed to recruit elements of the autophagy machinery through interactions between fungal HA and host cell CD44. Besides AMPK and AIC components, the endosomal and lysosomal markers EEA1, M6PR, and Cathepsin D, as well as the ER marker calreticulin, were also recruited to nascent phagosomes (Qin et al., 2011). Interestingly, co-localization of the endocytic marker EEA1 and the AIC component ULK1 was also observed, suggesting that the endosomal and lysosomal pathways, ER-derived membrane and selective autophagy machinery are involved in the internalization of Cn into host cells. How these factors coordinate this process and the involvement of other ubiquitin-binding autophagic adaptors related to the AIC remain to be characterized.

AMPK can be activated by cellular stresses that elevate AMP levels by means of allosteric binding of AMP to sites in the γ subunit AMPK, and by phosphorylation of Thr172 in AMPKα by the tumor suppressor LKB1, CaMKKβ, or the transforming growth factor-β-activated kinase (TAK1) (Hardie et al., 2012; Kola et al., 2006; Zadra et al., 2015). Activation of AMPK can induce autophagy via direct phosphorylation of ULK1 (Egan et al., 2011; Kim et al., 2011; Zhao and Klionsky, 2011). Previous observations showed that HA interactions with CD44 induces Ca^{2+} elevation in cells (Singleton and Bourguignon, 2002), and that increases in cytoplasmic Ca^{2+} concentrations induce autophagy through activation of CaMKKβ and AMPK pathways (Feng et al., 2020; Green et al., 2011). Similarly, our findings demonstrate that infection by Cn recruits host cell CD44 to CnCVs, induces intracellular Ca^{2+}-flux in the infected host cells, activates CaMKKβ and AMPK, and recruits AIC components to forming or nascent CnCVs. Cn infection also activates LKB1, and depletion of LKB1 reduced Cn internalization into host cells (Pandey et al., 2017). However, how the interaction of HA and CD44 activates AMPK through the upstream regulatory proteins LKB1 and TAK1 remains to be further characterized.

Our data support a stepwise model in which several sequential molecular events control the internalization of Cn in macrophages. First, interactions between fungal HA and CD44 on the surface of host cells likely stimulates the release of Ca^{2+} and elevates intercellular Ca^{2+} levels, which results in the activation of CaMKKβ and AMPK. Second, phosphorylation of ULK1 occurs in an AMPK-dependent fashion. Third, AMPK-dependent activation of ULK1 recruits AIC components, including the ULK1-ATG13-FIP200 complex, ATG9, and LC3, to the site of forming phagocytic cups containing the fungus. Fourth, the coordinated activities of AIC components drive the

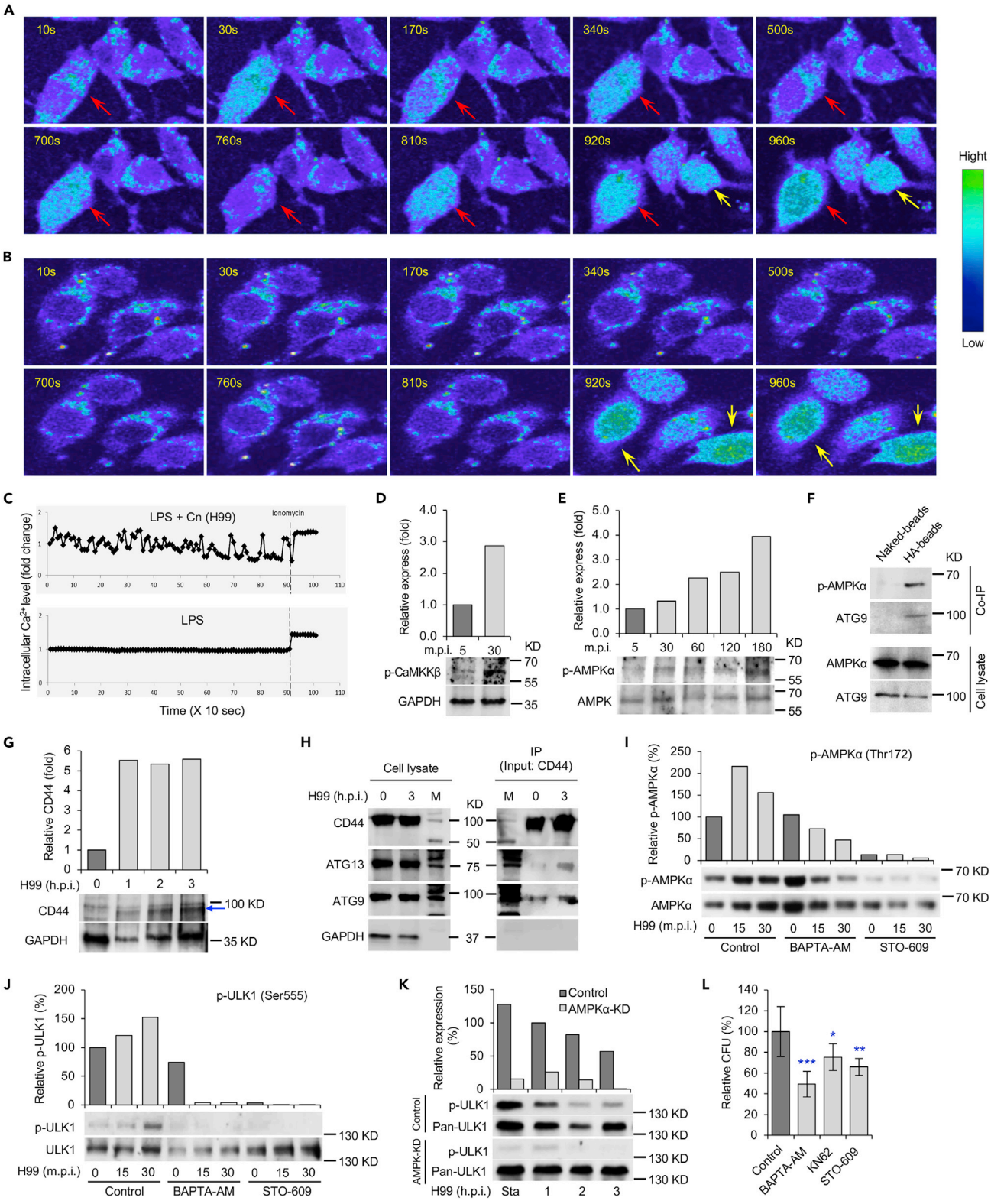

Figure 4. Cn infection activates CaMKKβ-AMPK-ULK1 signaling axis

(A and B) Cn infection results in intracellular Ca^{2+}-flux in the infected host cells. Host cells incubated with *cps1*$^{+}$ Cn (A) or PBS (B) and the intracellular Ca^{2+} level was detected by fluorescence emission between 500 and 550 nm. Red arrows: Intracellular Ca^{2+} increase in *cps1*$^{+}$-Cn-infected host

Figure 4. *Continued*

cells. Yellow arrows: Ca^{2+} releases from cells treated with ionomycin, a membrane permeable calcium ionophore used to increase intracellular calcium levels.

(C) Mean intracellular Ca^{2+} flux intensity of Cn-infected (upper panel) and control (lower panel) cells.

(D and E) Activation of host CaMKKβ (D) and AMPKα (E) in cells incubated with HA or HA-coated beads. Representative blots and data from one of three independent experiments are shown in (D to K).

(F) Co-immunoprecipitation (Co-IP) assays of host phosphorylated AMPKα and ATG9 trigged by HA-coated beads. Host cells were incubated with naked or HA-coated beads. At 3 h.p.i., the cells were lysed and immunoprecipitated using antibodies against CD44. The precipitated material was then visualized by Western blot analysis using antibodies directed against p-AMPKα or ATG9.

(G) Induction of CD44 protein (blue arrow) level by Cn infection. Host cells were infected with Cn H99 and at the indicated h.p.i., the infected cells were lysed and then subjected to immunoblotting assays using antibodies against CD44 and GAPDH.

(H) Co-IP assays show physical interactions between host CD44 and AIC components ATG13 or ATG9. BMDMs were infected with Cn H99 and at the indicated h.p.i., the infected cells were lysed and immunoprecipitated using antibodies against CD44. The precipitated material was then subjected to Western blot analysis using antibodies directed against CD44, ATG13 or ATG9. M: Prestained Protein Molecular Weight Marker.

(I and J) Chelation of intracellular Ca^{2+} by BAPTA-AM and inhibition of the activity of CaMKKβ by STO-609 reduce activation of AMPKα (I) and ULK1 (J). RAW264.7 macrophages were infected with Cn H99 in the absence or presence of BAPTA-AM (7.5 μM) or STO-609 (5 μM). At the indicated time points post infection, the infected cells were lysed for Western blot analysis using antibodies directed against p-AMPKα, p-ULK1, and pan-AMPKα or pan-ULK1.

(K) Depletion of AMPKα reduces activation of ULK1 during Cn internalization. Sta: starvation.

(L) Cn internalization in host cells treated by the indicated drug (BAPTA-AM: 7.5 μM, KN62: 5μM, STO-609: 5 μM) via CFU assays. Data represent the means ± SEM from three independent experiments. *, **, ***: significance at $p < 0.05$, 0.01, and 0.001, respectively.

internalization of the pathogen into host cells. ATG13 and FIP200 facilitate ULK1 to the site of autophagosome formation, kinase activity enhancement, and stability (Ganley et al., 2009). ULK1 kinase functions early in autophagy by regulating the outgrowth of autophagosomal membranes. Direct ULK1 phosphorylation of ATG9 is essential for autophagy and phosphorylated ATG9 is then required for the efficient recruitment of Atg8/LC3 and ATG18 to the sites of autophagosome formation and subsequent expansion of the isolation membrane (Papinski et al., 2014). Besides AIC and LC3, other autophagy proteins, e.g., ATG5, ATG12, may also be recruited to contribute to the elongation of phagosome membranes to envelop Cn in host cells; depletion or conditional-knockout of these proteins results in reduced Cn phagocytosis, intracellular replication, nonlytic exocytosis (Qin et al., 2011) or a less intense pneumonia and later alternative activation (Nicola et al., 2012). Ultimately, AIC component interactions with CnCVs gradually diminish as the pathogen establishes a replicative niche in host cells (Figure for graphical Abstract).

Finally, it is notable that several proteins in AMPKα and AIC regulatory networks are targets of commonly prescribed drugs (e.g., AMPK, a target for metformin) or under development as targets for pharmaceutical intervention (e.g., ULK1) (Egan et al., 2015). Several fungi, including *Candida* spp. and *Histoplasma capsulatum*, are capable of intracellular parasitism (Garcia-Rodas et al., 2011; Howard, 1965; Woods, 2003). Therefore, our findings may open up new therapeutic possibilities for preventing cryptococcosis and other infections caused by intracellular pathogens.

Limitations of the study

This study reveals fungal HA and host CD44 interactions activate a Ca^{2+}-CaMKKβ-AMPK-ULK1 signaling pathway that recruits autophagy initiation complex components, including AMPKα, ULK1, ATG13, FIP200 and ATG9, to forming phagosomes to drive fungal internalization. However, our understanding of how CD44 is recruited to phagocytic cups and how it coordinates with other components to promote Cn phagocytosis remains incomplete. It has been noted that the mobility of CD44 is dependent on the state of the actin cytoskeleton and the lipid composition of the plasma membrane (Jong et al., 2008). Our unpublished data imply that Toll-like receptors and mitogen-activated protein (MAP) kinase pathway activity may also be involved in the recruitment of AIC components and/or the induction of autophagy, processes which are mediated by HA-CD44 interactions. Further investigation is needed to address and clarify these remaining questions.

Resource availability

Lead contact

Further information and requests for resources and reagents should be directed to and will be fulfilled by the Lead Contact, Paul de Figueiredo (pjdefigueiredo@tamu.edu).

Materials availability

This study did not generate new unique reagents.

Data and code availability

This study did not generate/analyze datasets or code.

METHODS

All methods can be found in the accompanying Transparent Methods supplemental file.

SUPPLEMENTAL INFORMATION

Supplemental information can be found online at https://doi.org/10.1016/j.isci.2021.102192.

ACKNOWLEDGMENTS

We gratefully thank Dr. Arturo Casadevall (Department of Microbiology and Immunology, School of Medicine, Johns Hopkins University) for anti-cryptococcal antibodies, Dr. Jong (University of California, Los Angeles) for Cn strains C177, *cps1*Δ, and C558, and Steve Fullwood and Kalli Landua (Nikon Instruments) for expert assistance with the microscopy analysis. This work was supported by the Texas A&M Clinical Science Translational Research Institute Pilot Grant CSTR2016-1, the Defense Advanced Research Projects Agency (DARPA) (HR001118A0025-FoF-FP-006), NIH (R21AI139738-01A1, 1 R01AI141607-01A1, 1R21GM132705-01), the National Science Foundation (DBI 1532188, NSF0854684) and the Bill Melinda Gates Foundation to PdF; NIH grant awards NIH 1R01 AI48496-01A1 and NIH 1U54AI057156-0100 to TAF; the National Natural Science Foundation of China (# 81371773) to QMQ. Any opinions, findings, and conclusions or recommendations expressed in this material are those of the author(s) and do not necessarily reflect the views of the funding agencies.

AUTHOR CONTRIBUTIONS

P.D., Q.M.Q., T.A.F. designed the experiments. S.L.D., J.Y., X.F., Q.M.Q, A.P., R.M. D.Z., S.L.B., L.F.d.C. performed experiments. P.D., T.A.F., Q.M.Q., A.R., R.M., R.O.W., K.L.P. provided reagents/analysis tools. P.D., Q.M.Q., S.L.D., X.F., A.P., Y.L., T.A.F. analyzed data. P.D., Q.M.Q. supervised the work and wrote the manuscript. All authors read approved the final manuscript.

DECLARATION OF INTERESTS

The authors declare no competing interests.

Received: May 11, 2020
Revised: January 6, 2021
Accepted: February 9, 2021
Published: March 19, 2021

REFERENCES

Abada, A., and Elazar, Z. (2014). Getting ready for building: signaling and autophagosome biogenesis. EMBO Rep. *15*, 839–852.

Case, E.D.R., Smith, J.A., Ficht, T.A., Samuel, J.E., and de Figueiredo, P. (2016). Space: a final frontier for vacuolar pathogens. Traffic *17*, 461–474.

de Figueiredo, P., and Dickman, M. (2016). Plant disease: autophagy under attack. Elife *5*, e14447.

de Figueiredo, P., Ficht, T.A., Rice-Ficht, A., Rossetti, C.A., and Adams, L.G. (2015). Pathogenesis and immunobiology of brucellosis: review of Brucella–Host Interactions. Am. J. Pathol. *185*, 1505–1517.

Dickman, M., Williams, B., Li, Y., de Figueiredo, P., and Wolpert, T. (2017). Reassessing apoptosis in plants. Nat. Plants *3*, 773–779.

Egan, D.F., Chun, M.G., Vamos, M., Zou, H., Rong, J., Miller, C.J., Lou, H.J., Raveendra-Panickar, D., Yang, C.C., Sheffler, D.J., et al. (2015). Small molecule inhibition of the autophagy kinase ULK1 and identification of ULK1 substrates. Mol. Cell *59*, 285–297.

Egan, D.F., Shackelford, D.B., Mihaylova, M.M., Gelino, S., Kohnz, R.A., Mair, W., Vasquez, D.S., Joshi, A., Gwinn, D.M., and Taylor, R. (2011). Phosphorylation of ULK1 (hATG1) by AMP-activated protein kinase connects energy sensing to mitophagy. Science *331*, 456–461.

Evans, R.J., Sundaramurthy, V., and Frickel, E.-M. (2018). The interplay of host autophagy and eukaryotic pathogens. Front. Cell Dev. Biol. *6*, 118.

Feng, N., Wang, B., Cai, P., Zheng, W., Zou, H., Gu, J., Yuan, Y., Liu, X., Liu, Z., and Bian, J. (2020). ZEA-induced autophagy in TM4 cells was mediated by the release of Ca2+ activates CaMKKβ-AMPK signaling pathway in the endoplasmic reticulum. Toxicol. Lett. *323*, 1–9.

Galluzzi, L., Baehrecke, E.H., Ballabio, A., Boya, P., Bravo-San Pedro, J.M., Cecconi, F., Choi, A.M., Chu, C.T., Codogno, P., and Colombo, M.I. (2017). Molecular definitions of autophagy and related processes. EMBO J. *36*, 1811–1836.

Ganley, I.G., Lam, D.H., Wang, J., Ding, X., Chen, S., and Jiang, X. (2009). ULK1· ATG13· FIP200 complex mediates mTOR signaling and is essential for autophagy. J. Biol. Chem. *284*, 12297–12305.

Garcia-Rivera, J., Chang, Y.C., Kwon-Chung, K.J., and Casadevall, A. (2004). Cryptococcus neoformans CAP59 (or Cap59p) is involved in the extracellular trafficking of capsular glucuronoxylomannan. Eukaryot. Cell *3*, 385–392.

Garcia-Rodas, R., Gonzalez-Camacho, F., Rodriguez-Tudela, J.L., Cuenca-Estrella, M., and Zaragoza, O. (2011). The interaction between Candida krusei and murine macrophages results in multiple outcomes, including intracellular survival and escape from killing. Infect. Immun. *79*, 2136–2144.

Garcia-Rodas, R., and Zaragoza, O. (2012). Catch me if you can: phagocytosis and killing avoidance by Cryptococcus neoformans. FEMS Immunol. Med. Microbiol. *64*, 147–161.

Green, M.F., Anderson, K.A., and Means, A.R. (2011). Characterization of the CaMKKβ–AMPK signaling complex. Cell Signal. *23*, 2005–2012.

Guerra, C.R., Seabra, S.H., de Souza, W., and Rozental, S. (2014). Cryptococcus neoformans is internalized by receptor-mediated or 'triggered' phagocytosis, dependent on actin recruitment. PLoS One *9*, e89250.

Hardie, D.G., Ross, F.A., and Hawley, S.A. (2012). AMPK: a nutrient and energy sensor that maintains energy homeostasis. Nat. Rev. Mol. Cell Biol. *13*, 251–262.

Hosokawa, N., Hara, T., Kaizuka, T., Kishi, C., Takamura, A., Miura, Y., Iemura, S.-i., Natsume, T., Takehana, K., and Yamada, N. (2009). Nutrient-dependent mTORC1 association with the ULK1–Atg13–FIP200 complex required for autophagy. Mol. Biol. Cell *20*, 1981–1991.

Howard, D.H. (1965). Intracellular growth of Histoplasma capsulatum. J. Bacteriol. *89*, 518–523.

Irving, A.T., Mimuro, H., Kufer, T.A., Lo, C., Wheeler, R., Turner, L.J., Thomas, B.J., Malosse, C., Gantier, M.P., Casillas, L.N., et al. (2014). The immune receptor NOD1 and kinase RIP2 interact with bacterial peptidoglycan on early endosomes to promote autophagy and inflammatory signaling. Cell Host Microbe *15*, 623–635.

Johnston, S.A., and May, R.C. (2010). The human fungal pathogen Cryptococcus neoformans escapes macrophages by a phagosome emptying mechanism that is inhibited by Arp2/3 complex-mediated actin polymerisation. PLoS Pathog. *6*, e1001041.

Johnston, S.A., and May, R.C. (2013). Cryptococcus interactions with macrophages: evasion and manipulation of the phagosome by a fungal pathogen. Cell Microbiol. *15*, 403–411.

Jong, A., Wu, C.H., Chen, H.M., Luo, F., Kwon-Chung, K.J., Chang, Y.C., Lamunyon, C.W., Plaas, A., and Huang, S.H. (2007). Identification and characterization of CPS1 as a hyaluronic acid synthase contributing to the pathogenesis of Cryptococcus neoformans infection. Eukaryot. Cell *6*, 1486–1496.

Jong, A., Wu, C.H., Gonzales-Gomez, I., Kwon-Chung, K.J., Chang, Y.C., Tseng, H.K., Cho, W.L., and Huang, S.H. (2012). Hyaluronic acid receptor CD44 deficiency is associated with decreased Cryptococcus neoformans brain infection. J. Biol. Chem. *287*, 15298–15306.

Jong, A., Wu, C.H., Shackleford, G.M., Kwon-Chung, K.J., Chang, Y.C., Chen, H.M., Ouyang, Y., and Huang, S.H. (2008). Involvement of human CD44 during Cryptococcus neoformans infection of brain microvascular endothelial cells. Cell Microbiol. *10*, 1313–1326.

Jung, C.H., Jun, C.B., Ro, S.-H., Kim, Y.-M., Otto, N.M., Cao, J., Kundu, M., and Kim, D.-H. (2009). ULK-Atg13-FIP200 complexes mediate mTOR signaling to the autophagy machinery. Mol. Biol. Cell *20*, 1992–2003.

Khandia, R., Dadar, M., Munjal, A., Dhama, K., Karthik, K., Tiwari, R., Yatoo, M., Iqbal, H., Singh, K.P., and Joshi, S.K. (2019). A comprehensive review of autophagy and its various roles in infectious, non-infectious, and lifestyle diseases: current knowledge and prospects for disease prevention, novel drug design, and therapy. Cells *8*, 674.

Kim, J., Kundu, M., Viollet, B., and Guan, K.-L. (2011). AMPK and mTOR regulate autophagy through direct phosphorylation of Ulk1. Nat. Cell Biol. *13*, 132–141.

Kirkin, V., and Rogov, V.V. (2019). A diversity of selective autophagy receptors determines the specificity of the autophagy pathway. Mol. Cell *76*, 268–285.

Kola, B., Boscaro, M., Rutter, G.A., Grossman, A.B., and Korbonits, M. (2006). Expanding role of AMPK in endocrinology. Trends Endocrinol. Metab. *17*, 205–215.

Kozubowski, L., and Heitman, J. (2012). Profiling a killer, the development of Cryptococcus neoformans. FEMS Microbiol. Rev. *36*, 78–94.

Mack, H.I., Zheng, B., Asara, J.M., and Thomas, S.M. (2012). AMPK-dependent phosphorylation of ULK1 regulates ATG9 localization. Autophagy *8*, 1197–1214.

Nicola, A.M., Albuquerque, P., Martinez, L.R., Dal-Rosso, R.A., Saylor, C., De Jesus, M., Nosanchuk, J.D., and Casadevall, A. (2012). Macrophage autophagy in immunity to Cryptococcus neoformans and Candida albicans. Infect. Immun. *80*, 3065–3076.

O'Meara, T.R., and Alspaugh, J.A. (2012). The Cryptococcus neoformans capsule: a sword and a shield. Clin. Microbiol. Rev. *25*, 387–408.

Olszewski, M.A., Zhang, Y., and Huffnagle, G.B. (2010). Mechanisms of cryptococcal virulence and persistence. Future Microbiol. *5*, 1269–1288.

Pandey, A., Ding, S.L., Qin, Q.M., Gupta, R., Gomez, G., Lin, F., Feng, X., Fachini da Costa, L., Chaki, S.P., Katepalli, M., et al. (2017). Global reprogramming of host kinase signaling in response to fungal infection. Cell Host Microbe *21*, 637–649 e636.

Pandey, A., Lin, F., Cabello, A.L., da Costa, L.F., Feng, X., Feng, H.-Q., Zhang, M.-Z., Iwawaki, T., Rice-Ficht, A., and Ficht, T.A. (2018). Activation of host IRE1α-dependent signaling axis contributes the intracellular parasitism of Brucella melitensis. Front. Cell Infect. Microbiol. *8*, 103.

Papinski, D., Schuschnig, M., Reiter, W., Wilhelm, L., Barnes, C.A., Maiolica, A., Hansmann, I., Pfaffenwimmer, T., Kijanska, M., Stoffel, I., et al. (2014). Early steps in autophagy depend on direct phosphorylation of Atg9 by the Atg1 kinase. Mol. Cell *53*, 471–483.

Qin, Q.M., Luo, J., Lin, X., Pei, J., Li, L., Ficht, T.A., and de Figueiredo, P. (2011). Functional analysis of host factors that mediate the intracellular lifestyle of Cryptococcus neoformans. PLoS Pathog. *7*, e1002078.

Rubinsztein, D.C., Shpilka, T., and Elazar, Z. (2012). Mechanisms of autophagosome biogenesis. Curr. Biol. *22*, R29–R34.

Sabiiti, W., and May, R.C. (2012). Mechanisms of infection by the human fungal pathogen Cryptococcus neoformans. Future Microbiol. *7*, 1297–1313.

Saha, D.C., Goldman, D.L., Shao, X., Casadevall, A., Husain, S., Limaye, A.P., Lyon, M., Somani, J., Pursell, K., Pruett, T.L., et al. (2007). Serologic evidence for reactivation of cryptococcosis in solid-organ transplant recipients. Clin. Vaccin. Immunol. *14*, 1550–1554.

Seider, K., Heyken, A., Luttich, A., Miramon, P., and Hube, B. (2010). Interaction of pathogenic yeasts with phagocytes: survival, persistence and escape. Curr. Opin. Microbiol. *13*, 392–400.

Shoham, S., Huang, C., Chen, J.M., Golenbock, D.T., and Levitz, S.M. (2001). Toll-like receptor 4 mediates intracellular signaling without TNF-alpha release in response to Cryptococcus neoformans polysaccharide capsule. J. Immunol. *166*, 4620–4626.

Singleton, P.A., and Bourguignon, L.Y. (2002). CD44v10 interaction with Rho-kinase (ROK) activates inositol 1, 4, 5-triphosphate (IP3) receptor-mediated Ca2+ signaling during hyaluronan (HA)-induced endothelial cell migration. Cell Motil. Cytoskeleton *53*, 293–316.

Taborda, C.P., and Casadevall, A. (2002). CR3 (CD11b/CD18) and CR4 (CD11c/CD18) are involved in complement-independent antibody-mediated phagocytosis of Cryptococcus neoformans. Immunity *16*, 791–802.

Thurston, T.L., Wandel, M.P., von Muhlinen, N., Foeglein, A., and Randow, F. (2012). Galectin 8 targets damaged vesicles for autophagy to defend cells against bacterial invasion. Nature *482*, 414–418.

Warkentien, T., and Crum-Cianflone, N.F. (2010). An update on Cryptococcus among HIV-infected patients. Int. J. STD AIDS *21*, 679–684.

Woods, J.P. (2003). Knocking on the right door and making a comfortable home: Histoplasma capsulatum intracellular pathogenesis. Curr. Opin. Microbiol. *6*, 327–331.

Yang, Y., Kitagaki, J., Dai, R.M., Tsai, Y.C., Lorick, K.L., Ludwig, R.L., Pierre, S.A., Jensen, J.P., Davydov, I.V., Oberoi, P., et al. (2007). Inhibitors of ubiquitin-activating enzyme (E1), a new class of potential cancer therapeutics. Cancer Res. *67*, 9472–9481.

Zadra, G., Batista, J.L., and Loda, M. (2015). Dissecting the dual role of AMPK in cancer: from experimental to human studies. Mol. Cancer Res. *13*, 1059–1072.

Zaragoza, O. (2019). Basic principles of the virulence of Cryptococcus. Virulence *10*, 490–501.

Zhao, M., and Klionsky, D.J. (2011). AMPK-dependent phosphorylation of ULK1 induces autophagy. Cell Metab. *13*, 119–120.

iScience, Volume *24*

Supplemental information

Interactions between fungal hyaluronic acid and host CD44 promote internalization by recruiting host autophagy proteins to forming phagosomes

Shengli Ding, Jing Yang, Xuehuan Feng, Aseem Pandey, Rola Barhoumi, Dongmei Zhang, Samantha L. Bell, Yue Liu, Luciana Fachini da Costa, Allison Rice-Ficht, Robert O. Watson, Kristin L. Patrick, Qing-Ming Qin, Thomas A. Ficht, and Paul de Figueiredo

Transparent Methods

Key resources table

REAGENT or RESOURCE	SOURCE	IDENTIFIER
Antibodies		
Mouse anti-*C. neoformans* 18B7	Dr. Arturo Casadevall, (Albert Einstein College of Medicine of Yeshiva University, NY, USA)	N/A
CD44 Antibody [IM7]	GeneTex, Inc. (North America)	Cat. #: GTX80086
Mouse anti-HCAM(CD44)	Santa Cruz Biotechnology, Inc. (Dallas, TX USA)	Cat. #: sc-7297
anti-pCaMKKβ	Cell Signaling Technology, Inc. (Danver, MA USA)	Cat. #:16737S
anti-CaMKKα	Santa Cruz Biotechnology, Inc. (Dallas, TX USA)	Cat. #: sc-11370/17827
anti-CaMKKβ	Santa Cruz Biotechnology, Inc. (Dallas, TX USA)	Cat. #: sc-271674
Rabbit anti-pAMPKα (Thr 172)	Cell Signaling Technology, Inc. (Danver, MA USA)	Cat. #: 2535
Rabbit anti-AMPKα	Cell Signaling Technology, Inc. (Danver, MA USA)	Cat. #: 5831
Rabbit-anti pULK1 (Ser 555)	Cell Signaling Technology, Inc. (Danver, MA USA)	Cat. #: 5869
Rabbit anti-ULK1	Santa Cruz Biotechnology, Inc. (Dallas, TX USA)	Cat. #: sc-33182
Rabbit anti-LC3	Santa Cruz Biotechnology, Inc. (Dallas, TX USA)	Cat. #: sc-134226
Rabbit anti-GAPDH	Santa Cruz Biotechnology, Inc. (Dallas, TX USA)	Cat. #: sc-25778
Atg9A (D4O9D) Rabbit mAb	Cell Signaling Technology, Inc. (Danver, MA USA)	Cat. #: 13509S
Rabbit anti-ATG13	Sigma-Aldrich, Inc. (St. Louis, MO USA)	Cat. #: SAB4200100
Atg13 (E1Y9V) Rabbit mAb	Cell Signaling Technology, Inc. (Danver, MA USA)	Cat. #: 13468S
Rabbit anti-FIP200	Proteintech Group, Inc. (Rosemont, IL USA)	Cat. #: 17250-1-AP
Rabbit anti-AMPKβ	Novus Biologicals, Inc. (Littleton, CO USA)	Cat. #: NBP1-87487
Rabbit anti-pLKB1 (Ser428)	Abcam, Inc. (Cambridge, MA USA)	Cat. #: Ab63473
Rabbit anti-pAMPK (Thr172)-PE	BIOSS, Inc. (Woburn, MA USA).	Cat. #: BS-4002RP
Rabbit anti-pATG1 (Ser556)-PE	BIOSS, Inc. (Woburn, MA USA)	Cat. #: ABIN746733
Fungal, Bacterial and Virus Strains		
C. neoformans strain H99	Dr. Xiaorong Lin (Texas A&M University, College Station, TX)	N/A
C. neoformans strain AI100-dsRed	Dr. Xiaorong Lin (Texas A&M University, College Station, TX)	N/A
C. neoformans strain cap59	Dr. Xiaorong Lin (Texas A&M University, College Station, TX)	N/A
C. neoformans strain C177	Dr. Jong, A. (University of California, Los Angeles, CA, USA)	N/A
C. neoformans strain *cps1*Δ	Dr. Jong, A. (University of California, Los Angeles, CA, USA)	N/A
C. neoformans strain C588	Dr. Jong, A. (University of California, Los Angeles, CA, USA)	N/A
Chemicals, Peptides, and Recombinant Proteins		
STO-609	Sigma-Aldrich, Inc. (St. Louis, MO USA)	Cat. #: S1318-5MG
BAPTA-AM	Sigma-Aldrich, Inc. (St. Louis, MO USA)	Cat. #: A1076-25MG
KN62	Sigma-Aldrich, Inc. (St. Louis, MO USA)	Cat. #: I2142-1MG
RIPA buffer	G-Biosciences (San Diego, CA USA)	Cat. #: 786-489
Phosphatase inhibitor cocktail 2	Sigma-Aldrich, Inc. (St. Louis, MO USA)	Cat. #: P5726
Phosphatase inhibitor cocktail 3	Sigma-Aldrich, Inc. (St. Louis, MO USA)	Cat. #: P0044
Amino-polystyrene Particles	Spherotech, Inc. (Lake Forest, IL, USA)	Cat #: AP-10-10
Hyaluronic acid	Santa Cruz Biotechnology, Inc. (Dallas, TX USA)	Cat #: sc-337865
EDC hydrochloride	Santa Cruz Biotechnology, Inc. (Dallas, TX USA)	CAS #: 25952-53-8

pENTR4-eGFP-C1 entry vector	Addgene (Cambridge, MA, USA)	Plasmid #17396
pLenti-PGK-Neo destination vector	Addgene (Cambridge, MA, USA)	Plasmid #19067
psPAX2	Addgene (Cambridge, MA, USA)	Plasmids #12260
pMD2G/VSV-G	Addgene (Cambridge, MA, USA)	Plasmids #12259
G418	Invivogen (San Diego, CA, USA)	Cat #: NC9227938
Lipofectamine™ 2000	Invitrogen (Carlsbad, CA, USA)	Cat #: 11668027
Critical Commercial Assays		
Phagocytosis Assay Kit (IgG FITC)	Cayman Chemical, Inc. (Ann Arbor, MI USA)	Cat. #: 500290
Fe-NTA column	Thermo Fischer Scientific (Waltham, MA USA)	Cat. #: 88300
Pierce ECL Plus chemiluminescence kit	Thermo Fischer Scientific (Waltham, MA USA)	Cat. #: 32132X3
Experimental Models: Cell Lines		
RAW264.7 cells	ATCC (Manassas, VA USA)	TIB-71
J774A.1 cells	ATCC (Manassas, VA USA)	TIB-67
GFP-Gal8 (RAW264.7 macrophages)	This work	NA
GFP-LC3 (RAW macrophages)	Dr. Douglas Green (St. Jude Children's Research Hospital, Pittburgh, PA USA)	NA
B6J2 cells	Dr. J. Suttles (University of Louisville, Louisville, KY USA)	(Sag et al., 2008)
B6J2 cells (AMPKα-DN)	Dr. J. Suttles (University of Louisville, Louisville, KY USA)	(Sag et al., 2008)
Experimental Models: Organisms/Strains		
C57BL/6 wild-type (WT) mice	Jackson Laboratories, Inc. (Bar Harbor, ME USA)	Stock No: 000664
CD44-KO mice (B6.129 (Cg)-*Cd44*^{tm1Hbg}/J)	Jackson Laboratories, Inc. (Bar Harbor, ME USA)	Stock #: 005085

Experimental model details

Bone marrow-derived macrophage harvest and cultivation

Bone marrow cells were collected from the femurs of littermate control and CD44 KO mice, and cultivated in L929-cell conditioned media [DMEM medium containing 20% L929 cell supernatant, supplemented with 10% (v/v) FCS, penicillin (100 U/ml), and streptomycin (100 U/ml)]. After 3 days of culture, non-adherent precursors were washed away and the retained cells were propagated in fresh L929-cell conditioned media for another 4 days. For experimentation, BMDMs were split in 24-well plates at a density of 2.5×10^5 cells per well in L929-cell conditioned media and cultured at 37°C with 5% CO_2 overnight before use.

Method Details

Cryptococcus Strains and Infection, cell Culture and colony formation unit (CFU) assay

Yeast forms of Cn cells were cultured on YPD (Difco™) agar plates and maintained on the plates for 4 to 5 days prior to experimentation. Mammalian cell lines were routinely incubated in DMEM supplemented with 10% FBS in a 5% CO_2 atmosphere at 37°C. Preparation of cryptococcal and host cells for infection as well as CFU assays that measured internalized Cn cells were performed as previously described (Qin et al., 2011; Pandey et al., 2017). For CFU assay, host cells were infected with antibody-opsonized Cn cells at a multiplicity of infection (MOI) of 1 or 10 for 3 hrs; for immunofluorescence microscopy analysis, host cells were infected with antibody-opsonized or non-opsonized Cn cells with an MOI of 5 (unless otherwise indicated) for 1 to 3 h. At the indicated h.p.i., the infected cells were harvested for CFU assays or fixed and performed immunofluorescence microscopy assays (see below). To heat-kill Cn for use in immunofluorescence microscopy assays, Cn cells were heat inactivated as previously described (Wang et al., 2019). Briefly, the suspension of Cn cells (2.5×10^8 Cn cells/ml) was aliquoted into 2.0 ml Eppendorf tubes and heated on a hot plate at 75°C for 90 min. The death of the Cn cells was confirmed by plating the heat-treated cell suspension on YPD agar plates.

Immunofluorescence microscopy assays for Cn phagocytosis

Mammalian host cells were first cultivated on 12 mm glass coverslips (Fisherbrand) on the bottom of 24-well plates (Falcon) for 12-16 h before infection. Next, the host cells were infected with the tested Cn cells and incubated at 37°C in a 5% CO_2 atmosphere. At the indicated time points post-infection, culture media was removed and the infected host cells were washed 6 to 8 times with PBS (pH 7.4) before being fixed with 3.7% formaldehyde. The fixed cells (at room temperature for 1 to 2 hrs) were then processed Cn phagocytosis assays using antibody (18B7) directed against Cn as previous described (Qin et al., 2011; Pandey et al., 2017) without adding Triton X-100 to the staining buffer. The numbers of internalized (unstained) and extracellular (stained) Cn cells were then quantified and plotted. Images represent a representative image from triplicate replicates, with 100 fields imaged per replicate.

Drug/compound treatments

Murine macrophage J774.A1 or RAW264.7 cells were overnight cultured in 48 well plates and then coincubated with assorted pharmacological compounds, including KN62 (5 μM), STO-609 (5 μM) or BAPTA-AM (7.5 μM) for 2 h. Cells treated with the solvent dimethyl sulfoxide (DMSO) for these compounds served as controls. The media containing the compounds was then

removed. For CFU assays, the drug-treated cells were extensively washed with fresh medium and then infected with Cn cells. At 3 h.p.i., the infected cells were lysed and performed CFU assay as previously described (Qin et al., 2011; Pandey et al., 2017). For western blots, the compound-treated cells were washed 3 times with cold 1 × PBS, pH7.4, lysed and performed immunoblotting assay as previously describe (Pandey et al., 2017).

Lentivirus-mediated depletion of host proteins

The pSuperRetro retrovirial vector system (OligoEngine, Inc.) was used to knockdown target gene expression in murine cells according to the manufacturer's instructions. The oligonucleotides used for shRNA construction to knockdown the expression of mouse genes and the accompanying references are listed in **Table S1**. Transfection was performed in 6-well plates containing 1.5×10^5 RAW264.7 or B6J2 cells. Clones with the insert stably integrated were selected with puromycin. Western blot was performed to validate the depletion of the targeted proteins. All Westerns were performed in triplicate and representative findings are shown.

Generation of GFP-tagged Gal8 RAW264.7 cells

The GFP-galectin-8 expression construct was made by first cloning the cDNA sequence of *Lgals8* (from RAW 264.7 cells) into the pENTR4-eGFP-C1 entry vector (Campeau et al., 2009), resulting in a fusion of eGFP on the N-terminus of galectin-8. This construct was fully Sanger sequenced (Eton Biosceinces, San Diego, CA) to verify the fusion protein was in-frame and error-free. GFP-Gal8 was then Gateway cloned with LR Clonase (Invitrogen) into the pLenti-PGK-Neo destination vector (Campeau et al., 2009). Lenti-X 293T cells (Takara Bio) were co-transfected with pLenti-GFP-Gal8 and the packaging plasmids psPAX2 and pMD2G/VSV-G (Addgene Plasmids #12259-60) to produce lentiviral particles. RAW 264.7 cells were transduced with GFP-Gal8 lentivirus for two consecutive days plus 1:1000 Lipofectamine 2000 (Invitrogen) and selected for 5 days with 750 μg/ml G418 (Invivogen). Expression of GFP-Gal8 was confirmed by Western blot analysis and fluorescence microscopy.

Confocal microscopy assays

Host cells were infected with live or heat killed, opsonized or unopsonized capsular or acapsular strains of Cn. At the indicated times post-infection, host cells were fixed for confocal immunofluorescence microscopy analysis using antibodies directed against the indicated host

proteins. Immunofluorescence microscopy staining and imaging methods (Qin et al., 2008; Qin et al., 2011; Pandey et al., 2017; Pandey et al., 2018) were used to determine the subcellular localization of host AIC components in infected host cells. Samples were observed on a laser scanning confocal microscope or on a confocal fluorescence microscope (ECLIPSE Ti, Nikon). Confocal images (1,024 × 1,024 pixels) were acquired and processed with NIS elements AR 3.0 software (Nikon) and assembled with Adobe Photoshop CC 2019 (Adobe Systems, CA, USA). Digital image analysis and quantification was performed as previously described (Qin et al., 2011). Findings from our subcellular localization analyses were not an artifact of secondary antibody cross reactivity with host or pathogen components because negligible fluorescence signal was observed when infected cells were stained with secondary antibodies alone, or the pathogen alone was stained with the antibodies used in the experiments (**Figure S5G**).

Protein pull-down assays

For protein pull-down assay with HA-coated or naked beads, spherical amino polysterene beads (size: 1.0-1.4 µm, Spherotech Inc, IL, USA) were covalently coupled using EDC [*N*-Ethyl-*N*′-(3-dimethylaminopropyl)carbodiimide hydrochloride] to hyaluronic acid (HA) (Santa Cruz Biotec.) as per the manufacturer's (Spherotech) instruction. Briefly, 200 µl of 0.05 M sodium acetate buffer (pH 5.0), 2 mg of HA, 2 ml of 5% w/v Amino particles and 20 mg of EDC were mixed in a glass centrifuge tube. The contents were vortexed and incubated for 2 hrs at ambient temperature on a rotary mixer. Following incubation, the tube was centrifuged at 3000 × g for 15 minutes and supernatant was carefully discarded. The pellet was washed twice in 1 × PBS and resuspended in 2 ml of 1 × PBS to obtain 5% w/v suspension of HA coated beads. RAW 264.7 cells (3×10^5) were washed with 1 × PBS. Next, a bead incubation solution containing 5 µl of HA-coated or naked beads in 200 µl of PBS was added to the washed cells. The cells were centrifuged for 10 min at 1500 RPM and then incubated in a humidified incubator containing 5% CO_2 for 2 hrs. The treated cells were washed 2-4 times with ice-cold 1 × PBS and lysed in 80 µl RIPA buffer supplemented with a cocktail of protease and phosphatase inhibitors. Beads were separated from the lysate by high-speed centrifugation at 4°C. The separated beads were washed 3 times with RIPA buffer and finally resuspended in 80 µl RIPA buffer and 20 µl of 5 × sample buffer (Thermo Scientific) and boiled for 5 mins. Samples were finally resolved by SDS-PAGE and subjected to western blot analysis.

For testing host CD44 physical interactions with AIC components during Cn infection, BMDMs were infected with H99 at an MOI of 10. At the indicated (0, 1, 2, 3) h.p.i., Cn infected cells were lysed. We then performed protein pull-down assays with CD44 as an input. The assays were performed using the Pierce Co-Immunoprecipitation (Co-IP) Kit (Thermo Scientific, USA) according to the manufacturer's instructions.

Immunoblotting analysis

Preparation of protein samples and western blot analysis were performed as described previously (Qin et al., 2011; Pandey et al., 2017; Pandey et al., 2018). Blot densitometry was performed using the ImageJ (http://rsbweb.nih.gov/ij/) software package. All Westerns were performed in triplicate and representative findings are shown.

Intracellular Ca^{2+} measurements

Measurement of intracellular Ca^{2+} levels of host cells infected with Cn cells, HA-treated and control cells were performed as the method previously described (Barhoumi et al., 2007). Briefly, cells were loaded for 1 h with 3.0 μM fluo4-AM at 37 °C in serum- and phenol red-free medium and then washed with the same medium. Fluo4-AM is a visible wavelength probe which exhibits about a 40 fold enhancement of fluorescence intensity upon Ca^{2+} binding (Gee et al., 2000). Fluo4-AM fluorescence was generated in the cells by argon laser excitation at 488 nm and fluorescence emission between 500 and 550 nm was monitored. Images were collected with Zeiss LSM 510 confocal microscope using a 63× objective/1.4 oil. Images presented have dimensions of 50 μm × 50 μm.

Quantification and statistical analysis

The quantitative data presented in this work represent the mean ± standard error of mean (SEM) from at least three independent experiments. To easily compare results from independent experiments, the data from controls, such as protein expression level, blot densitometry, CFU, intracellular Cn number, etc., were normalized as 1 or 100%. The significance of the data was assessed using the Student's *t*-test to assess statistical significance between two experimental groups or a one-way ANOVA test to evaluate the statistical differences of multiple comparisons of the data sets.

Supplemental Information

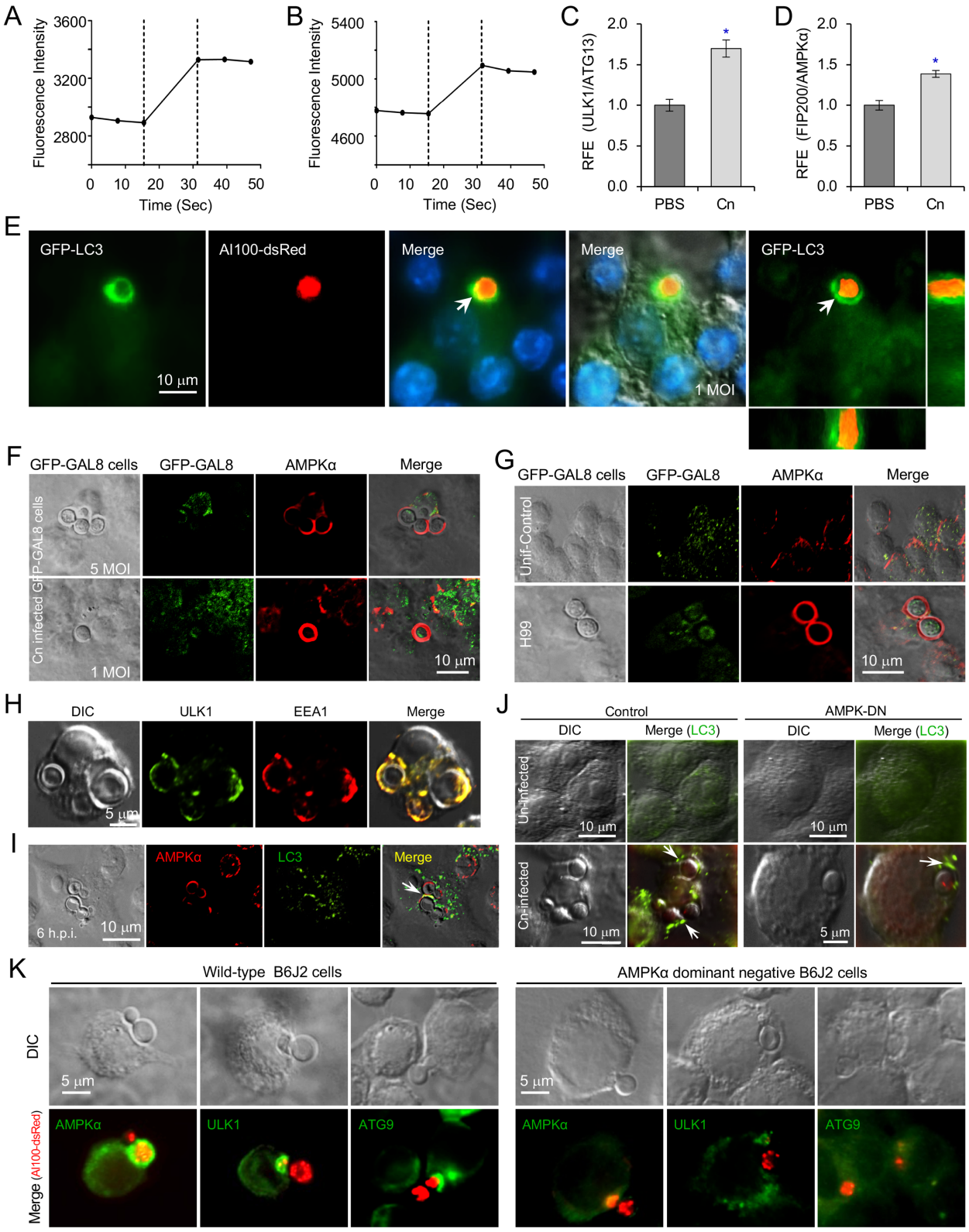

Figure S1. Recruitment of AIC components, but not galectin 8, to nascent phagosomes during *Cryptococcus neoformans* (Cn) internalization (Related to Figure 1).

The indicated host cells were infected with Cn cells at an MOI of 5. At 3 hrs post infection (h.p.i.), the infected host cells were fixed (3.7% formaldehyde in 1×PBS at room temperature for ~2 hrs) and subjected to Forster Resonance Energy Transfer (FRET) imaging microscopy (Irving et al., 2014; Wolf et al., 2013) or confocal immunofluorescence microscopy assays with the indicated antibodies.

(A, B) Fluorescence intensity of ULK1 and ATG13 (A) or FIP200 and AMPKα (B) during Cn internalization.

(C, D) Interactions between host ULK1 and ATG13 (C) or FIP200 and AMPKα (D) during recruitment to Cn-containing vacuoles (CnCVs) in RAW264.7 macrophages. The infected host cells were determined using FRET analysis. RFE: relative FRET-efficiency (between the FRET-pairs in the parentheses). The FRET-efficiency of Cn infected cells was compared to PBS control (normalized as 1). Data represent the means ± standard error of mean (SEM) from at least three independent experiments. *: significance at $p < 0.05$.

(E) Recruitment of host LC3 to nascent CnCVs during Cn (unopsonized) internalization.

(F, G) Host galectin 8 is not recruited to nascent phagosomes containing Cn cells during Cn internalization by host cells expressing GFP-galectin 8 (F) or cells supplemented with UBEI-41, a cell permeable inhibitor of ubiquitin-activating enzyme E1 (G).

(H) Colocalization of the host early endosomal marker EEA1 with AIC component ULK1 surrounding nascent CnCVs.

(I) Recruitment of host AMPKα and LC3 to nascent phagosomes containing Cn cells in infected bone marrow derived macrophages (BMDMs).

(J) Recruitment of host LC3 to nascent phagosomes containing Cn cells in infected or uninfected B6J2 macrophages expressing a dominant negative variant of AMPKα (AMPK-DN) or control.

(K) Less recruitment of host AMPKα and AIC component ULK1 or ATG9 to nascent CnCVs in B6J2 macrophages expressing an AMPK-DN variant during Cn internalization.

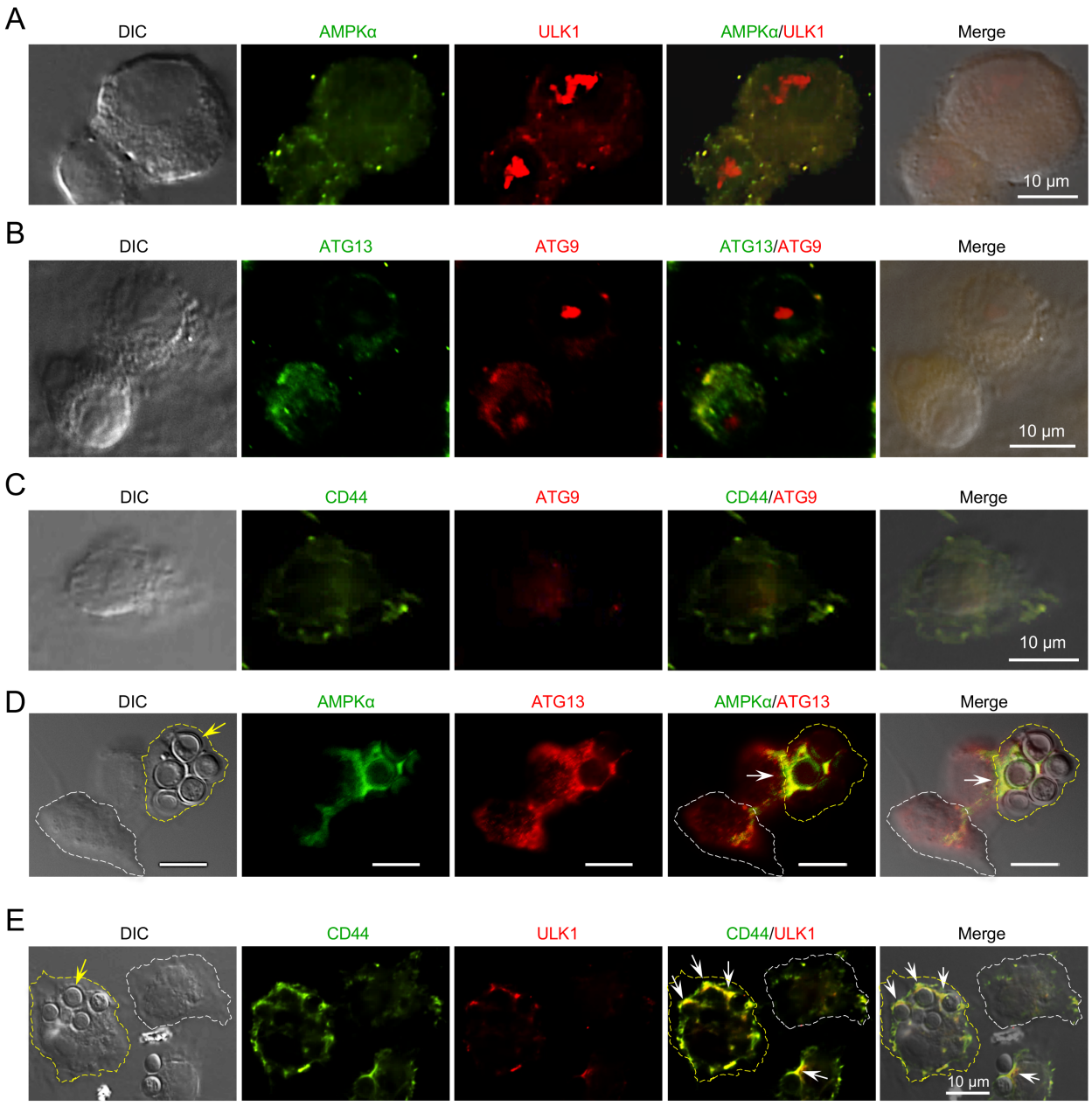

Figure S2. Expression and localization of the indicated host proteins in cells with or lacking Cn cells (Related to Figures 1, 2 and 3).

(A-C) Expression and localization of AMPKα and ULK1 (A), ATG9 and ATG13 (B), CD44 and ATG13 (C) in uninfected host cells.

(D, E) Comparison of the expression and localization of AMPKα and ATG13 (D, related to Figure 1A) or CD44 and ULK1 (E, related to Figure 3D) in Cn infected host cells containing or lacking Cn cells (bounded with yellow and white dash lines, respectively). Bars: 10 μm. Yellow arrows: Cn cells; white arrows: colocalization of the indicated proteins.

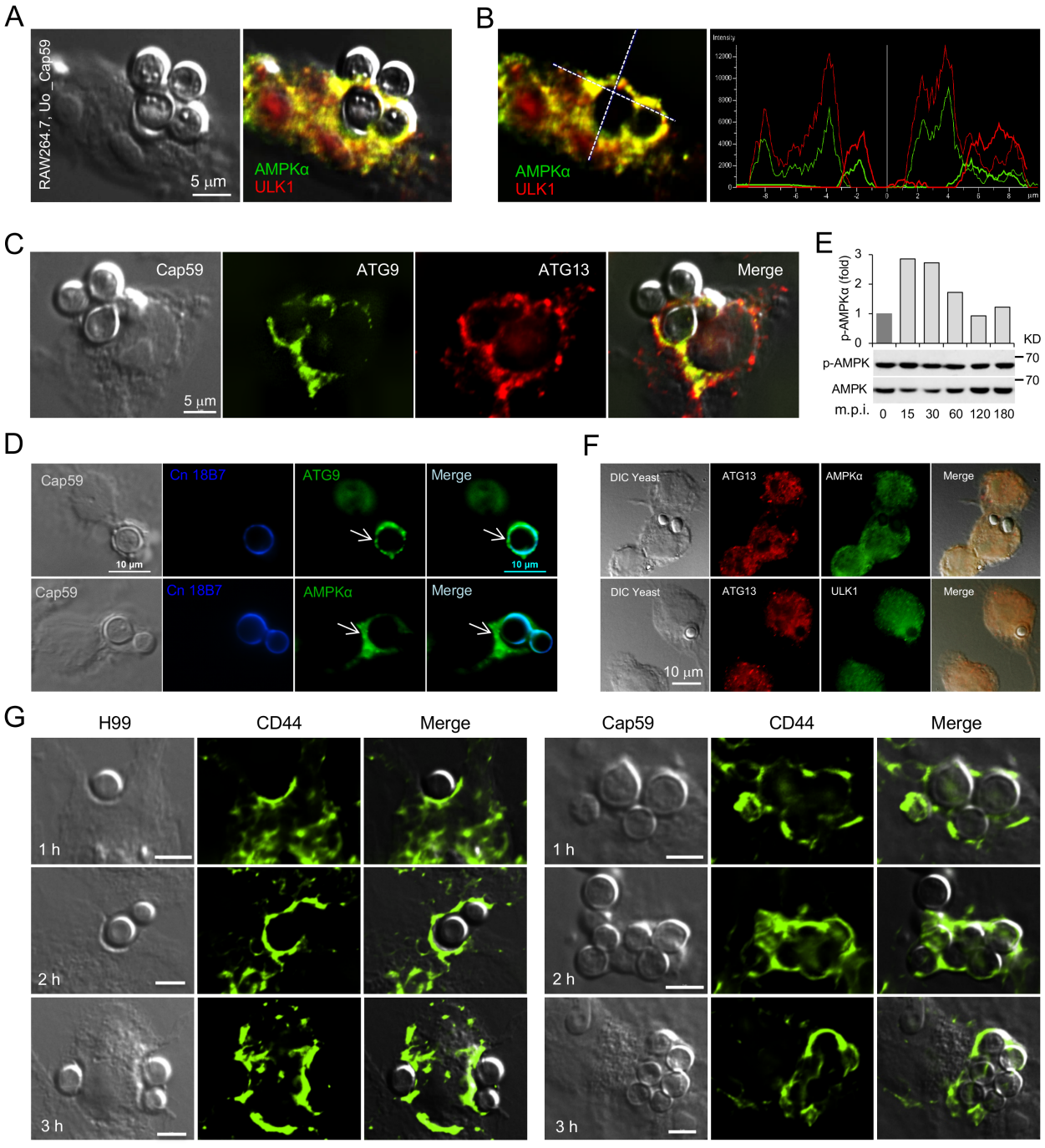
A
RAW264.7, Uo_Cap59
5 μm
AMPKα
ULK1
B
AMPKα
ULK1
Intensity
μm
C
Cap59
5 μm
ATG9
ATG13
Merge
E
p-AMPKα (fold)
KD
p-AMPK
AMPK
70
70
m.p.i.
0 15 30 60 120 180
D
Cap59
Cn 18B7
ATG9
Merge
10 μm
Cap59
Cn 18B7
AMPKα
Merge
F
DIC Yeast
ATG13
AMPKα
Merge
DIC Yeast
ATG13
ULK1
Merge
10 μm
G
H99
CD44
Merge
Cap59
CD44
Merge
1 h
2 h
3 h
1 h
2 h
3 h

Figure S3. Recruitment of host AIC components and CD44 to forming or nascent CnCVs during Cn internalization (Related to Figures 1, 2 and 3).

(A) Recruitment of AMPKα and AIC components ULK1 to nascent CnCVs. Uo_cap59: Unopsozied cap59.

(B) The fluorescence intensity profile of AMPKα and ULK1 along the two crossed white lines (left panel).

(C) Colocalization of ATG9 with ATG13 in the vicinities of CnCvs.

(D) Colocalization of host AMPKα or ATG9 with cryptococcal glucuronoxylomannan (GXM)-specific monoclonal antibody 18B7.

(E) Activation of host AMPKα by heat-killed (HK) Cn cells (cap 59) during phagocytosis. Representative results from one of three independent experiments are shown.

(F) Recruitment of AIC components and AMPKα to nascent phagosomes is minimally detected during phagocytosis of yeast (*Saccharomyces cerevisiae*) cells by host cells.

(G) Recruitment of CD44 during a time course (3 hr) of Cn internalization. Bars: 5 μm.

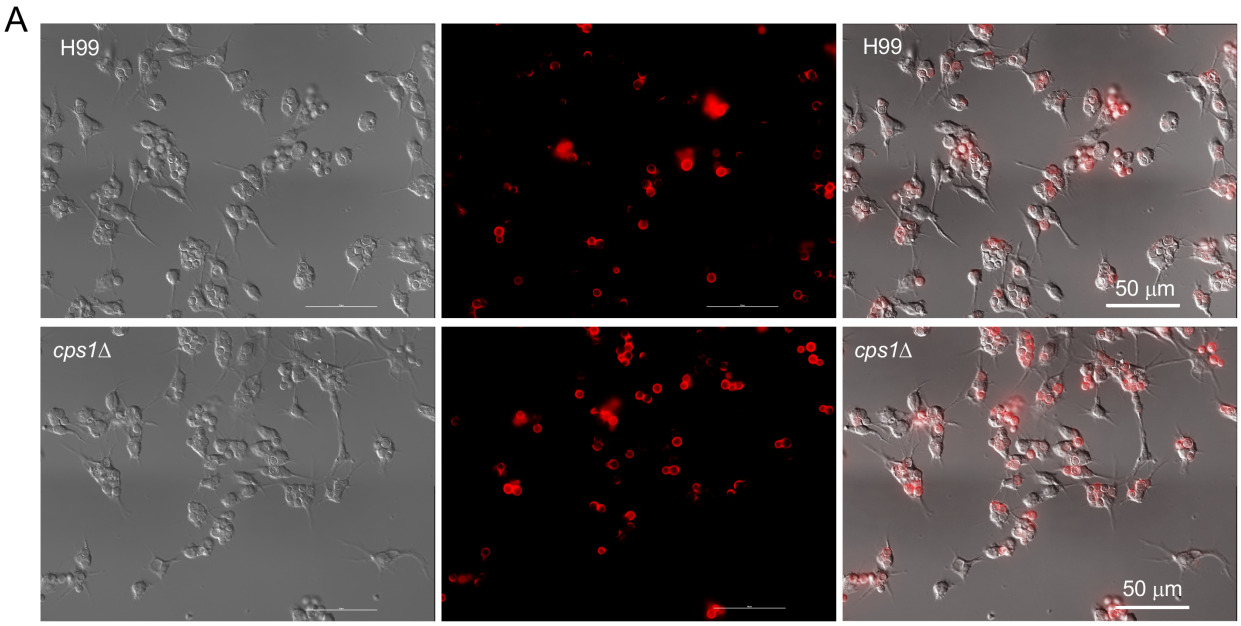
A
H99
H99
50 μm
cps1Δ
cps1Δ
50 μm

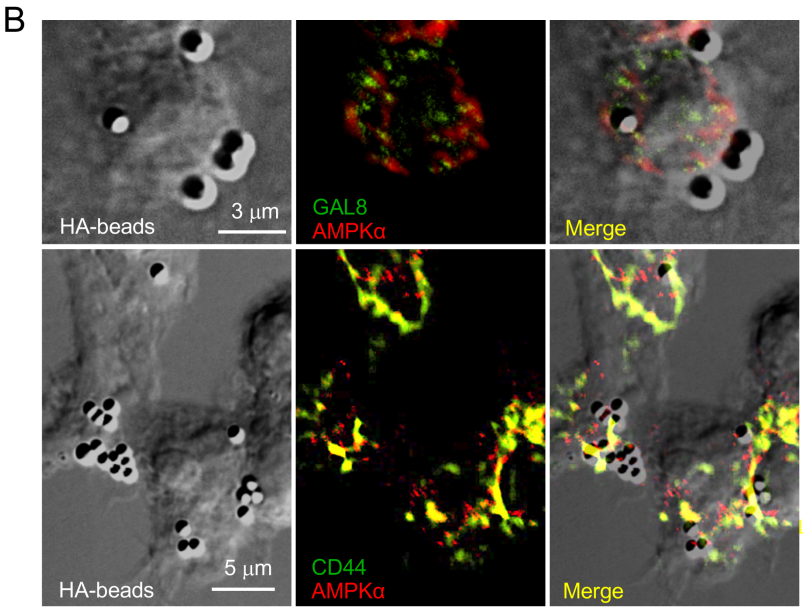
B
HA-beads
3 μm
GAL8
AMPKα
Merge
HA-beads
5 μm
CD44
AMPKα
Merge

Figure S4. Fungal hyaluronic acid (HA) is required for Cn internalization (Related to Figure 3).

(A) Disruption of Cn *cps1* impairs internalization of the fungal pathogen (related to Figure 3B-C). BMDMs were infected with the indicated Cn cells at an MOI of 10. At 3 h.p.i., the infected cells were fixed and then subjected to non-permeable immunofluorescence staining (Pandey et al., 2017) with Cn GXM-specific monoclonal antibody 18B7. Cn cells with red fluorescence represent incompletely internalized or extracellular Cn cells.

(B) Recruitment of CD44, not galectin 8, to the forming or nascent phagosomes associated with HA-coated beads. Upper panel: localization of galectin 8 (GAL8) and AMPKα in cells incubated with HA-coated beads. Lower panel: colocalization of CD44 and AMPKα to the forming or nascent phagosomes related to HA-coated beads.

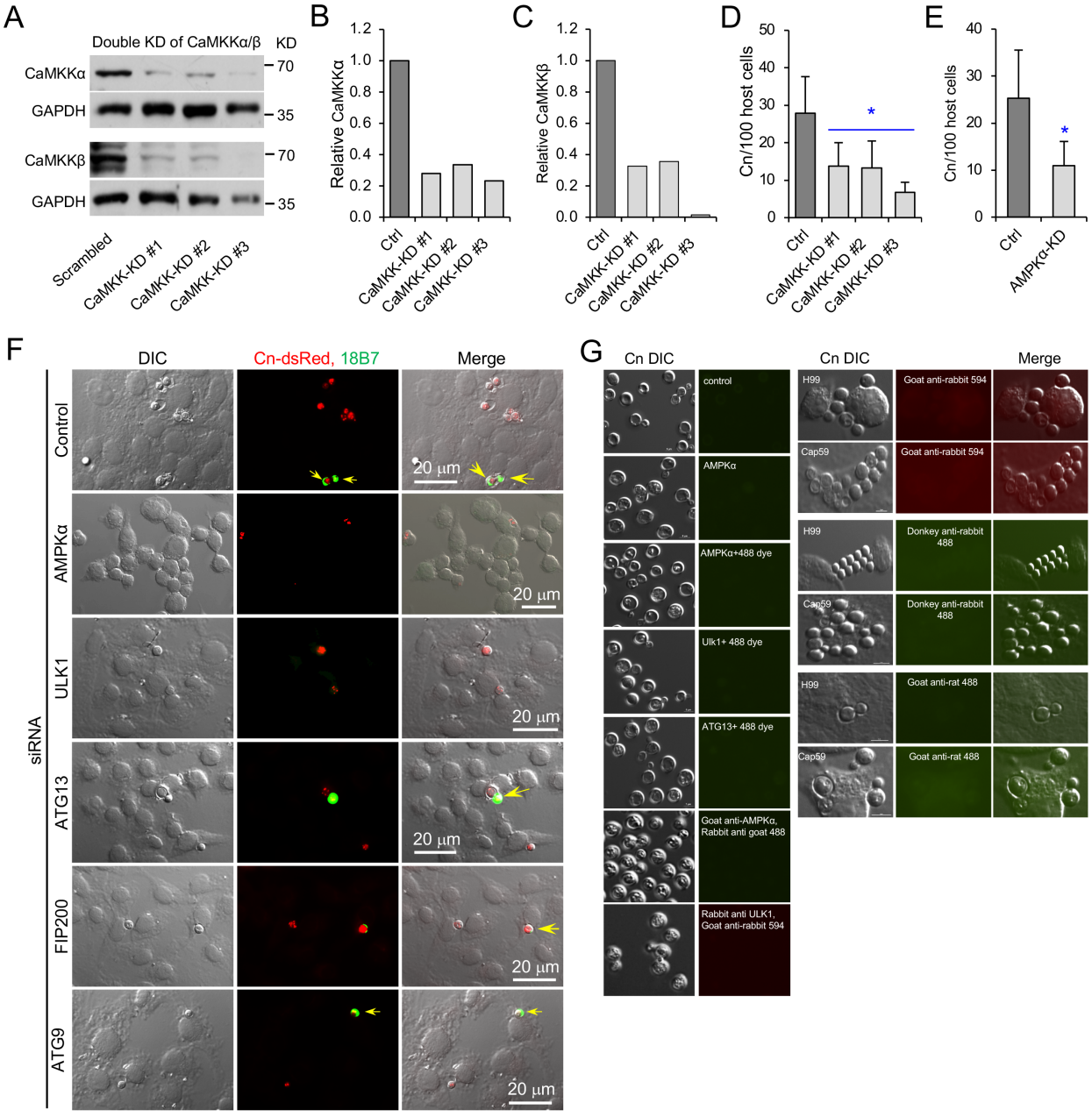
A
Double KD of CaMKKα/β
KD
CaMKKα
GAPDH
CaMKKβ
GAPDH
70
35
70
35
Scrambled
CaMKK-KD #1
CaMKK-KD #2
CaMKK-KD #3
B
Relative CaMKKα
C
Relative CaMKKβ
D
Cn/100 host cells
E
Cn/100 host cells
Ctrl
AMPKα-KD
F
DIC
Cn-dsRed, 18B7
Merge
siRNA
Control
AMPKα
ULK1
ATG13
FIP200
ATG9
20 μm
G
Cn DIC
control
AMPKα
AMPKα+488 dye
Ulk1+ 488 dye
ATG13+ 488 dye
Goat anti-AMPKα, Rabbit anti goat 488
Rabbit anti ULK1, Goat anti-rabbit 594
Cn DIC
Merge
H99
Cap59
Goat anti-rabbit 594
Donkey anti-rabbit 488
Goat anti-rat 488

Figure S5. Components in the CaMKK-AMPK-ULK1 signal axis play important roles in Cn internalization (Related to Figure 4).

(A) Immunoblotting assay to test the depletion of CaMKKα/β protein level by the shRNA approach.

(B, C) Relative protein expression levels of CaMKKα (B) or CaMKKβ (C) in RAW macrophages transfected with scrambled or CaMKKα/β shRNAs. Data from a representative experiment shown in (A). Ctrl: control.

(D, E) Depletion of host cell CaMKKα/β (D) or AMPKα (E) reduces Cn internalization determined by immunofluorescence microscopy assay. Data represent the means ± SEM from three independent experiments. *: significance at $p < 0.05$.

(F) Depletion of host cell AMPKα and AIC components reduces Cn internalization as determined using an immunofluorescence microscopy assay. Cn cells with green fluorescence represent incompletely internalized or extracellular Cn cells. Images from a representative experiment of three independent experiments.

(G) Cn cells harvested from infected host cells (leaf panel) or during host infection (right panel) do not display cross activities with the primary or secondary antibodies used in this work.

Table S1. shRNAs and PCR primers used in this study (Related to Figure 4, Figure S1, and Figure S4)

shRNA ID	Sequence (5'-3')	References
shCaMKKα 1	GGAAGTGCCCGTTCATTGATT	This study
shCaMKKα 2	TCAATGGCTGAGGTGAGGCAC	This study
shCaMKKβ1	GGTGCTGTCCAAAAAGAAA	This study
shCaMKKβ2	TTGCGTAATAAGTATTGTCAT	This study
shFIP200	GAGAGAACTTGTTGAGAAA	Pandey et al., 2017
	ACATGAAGGCTCAGAGAAA	ditto
shUlk1	GAGCAAGAGCACACGGAA A	ditto
	AGACTCCTGTGACACAGAT	ditto
shAtg13	GAGAAGAATGTCCGAGAAT	ditto
	ACAGGAAGGACTTGGACAA	ditto
shPrkaa1	TGAATTAAACCCACAGAAA	ditto
	GGTCATCAGTACACCATCT	ditto
shPrkab1	TGAACAAGGACACGGGCAT	ditto
	GCACGACCTGGAAGCGAAT	ditto
Scramble 1	ATTGTATGCGATCGCAGAC	ditto
Scramble 2	CACCAGCATCTGATCTAGA	ditto
Ulk1-F1	ACTGCGGCCGCatggattacaaggatgacgatgacaagatggag ccgggccgcggcggc	ditto
Ulk1-r1	GAAGAATTCtcaggcatagacaccactcag	ditto
ULK1-F2	GATCTGGATCCGGAGTCGACGGAGCGGCCGCatggatta caagga	ditto
Ulk1-R2	AGCGCCTCCCCTACCCGGTAGAATTCtcaggcatagaca ccactc	ditto
Atg13-F1	ACTAGATCTATGTACCCATACGATGTTCCAGATTACGCT ATGGAAACTGAACTCAGCTCC	ditto
Atg13-R1	GAACTCGAGTTACTGCAGGGTTTCCACAAA	ditto
Atg13-F2	ACTCCTTCTCTAGGCGCCGGAATTAGATCTATGTACCCA TACGAT	ditto
Atg13-R2	ACCCGGTAGAATTCGTTAACCTCGAGttactgcagggtt tccaca	ditto
Prkaa1-F1	ACTGCGGCCGCATGGTGAGCAAGGGCGAGGAGCTGTTCA	ditto
Prkaa1-R1	GAAGAATTCTTACTGTGCAAGAATTTTAAT	ditto
Prkaa1-F2	GATCTGGATCCGGAGTCGACGGAGCGGCCGCATGGTGAG CAAGGG	ditto
Prkaa1-R2	AGCGCCTCCCCTACCCGGTAGAATTCttactgtgcaaga atttta	ditto

Supplemental References

Barhoumi, R., Burghardt, R.C., Qian, Y., and Tiffany-Castiglioni, E. (2007). Effects of propofol on intracellular Ca2+ homeostasis in human astrocytoma cells. Brain Res *1145*, 11-18.

Campeau, E., Ruhl, V.E., Rodier, F., Smith, C.L., Rahmberg, B.L., Fuss, J.O., Campisi, J., Yaswen, P., Cooper, P.K., and Kaufman, P.D. (2009). A versatile viral system for expression and depletion of proteins in mammalian cells. PloS one *4*.

Gee, K.R., Brown, K., Chen, W.U., Bishop-Stewart, J., Gray, D., and Johnson, I. (2000). Chemical and physiological characterization of fluo-4 Ca2+-indicator dyes. Cell calcium *27*, 97-106.

Irving, A.T., Mimuro, H., Kufer, T.A., Lo, C., Wheeler, R., Turner, L.J., Thomas, B.J., Malosse, C., Gantier, M.P., Casillas, L.N.*, et al.* (2014). The immune receptor NOD1 and kinase RIP2 interact with bacterial peptidoglycan on early endosomes to promote autophagy and inflammatory signaling. Cell host & microbe *15*, 623-635.

Pandey, A., Ding, S.L., Qin, Q.M., Gupta, R., Gomez, G., Lin, F., Feng, X., Fachini da Costa, L., Chaki, S.P., Katepalli, M.*, et al.* (2017). Global Reprogramming of Host Kinase Signaling in Response to Fungal Infection. Cell host & microbe *21*, 637-649 e636.

Pandey, A., Lin, F., Cabello, A.L., da Costa, L.F., Feng, X., Feng, H.Q., Zhang, M.Z., Iwawaki, T., Rice-Ficht, A., Ficht, T.A.*, et al.* (2018). Activation of Host IRE1alpha-Dependent Signaling Axis Contributes the Intracellular Parasitism of Brucella melitensis. Front Cell Infect Microbiol *8*, 103.

Qin, Q.M., Luo, J., Lin, X., Pei, J., Li, L., Ficht, T.A., and de Figueiredo, P. (2011). Functional analysis of host factors that mediate the intracellular lifestyle of Cryptococcus neoformans. PLoS Pathog *7*, e1002078.

Qin, Q.M., Pei, J., Ancona, V., Shaw, B.D., Ficht, T.A., and de Figueiredo, P. (2008). RNAi screen of endoplasmic reticulum-associated host factors reveals a role for IRE1alpha in supporting Brucella replication. PLoS Pathog *4*, e1000110.

Sag, D., Carling, D., Stout, R.D., and Suttles, J. (2008). Adenosine 5'-monophosphate-activated protein kinase promotes macrophage polarization to an anti-inflammatory functional phenotype. Journal of immunology *181*, 8633-8641.

Wang, Y., Wang, K., Masso-Silva, J.A., Rivera, A., and Xue, C. (2019). A Heat-Killed Cryptococcus Mutant Strain Induces Host Protection against Multiple Invasive Mycoses in a Murine Vaccine Model. mBio *10*.

Wolf, A., Akrap, N., Marg, B., Galliardt, H., Heiligentag, M., Humpert, F., Sauer, M., Kaltschmidt, B., Kaltschmidt, C., and Seidel, T. (2013). Elements of transcriptional machinery are compatible among plants and mammals. PLoS One *8*, e53737.